Photonik
Ingenieurbüro
Dr. Walter Luhs

PE-1600 Iodine Molecular Spectroscopy and LE-1300 Iodine Raman Laser

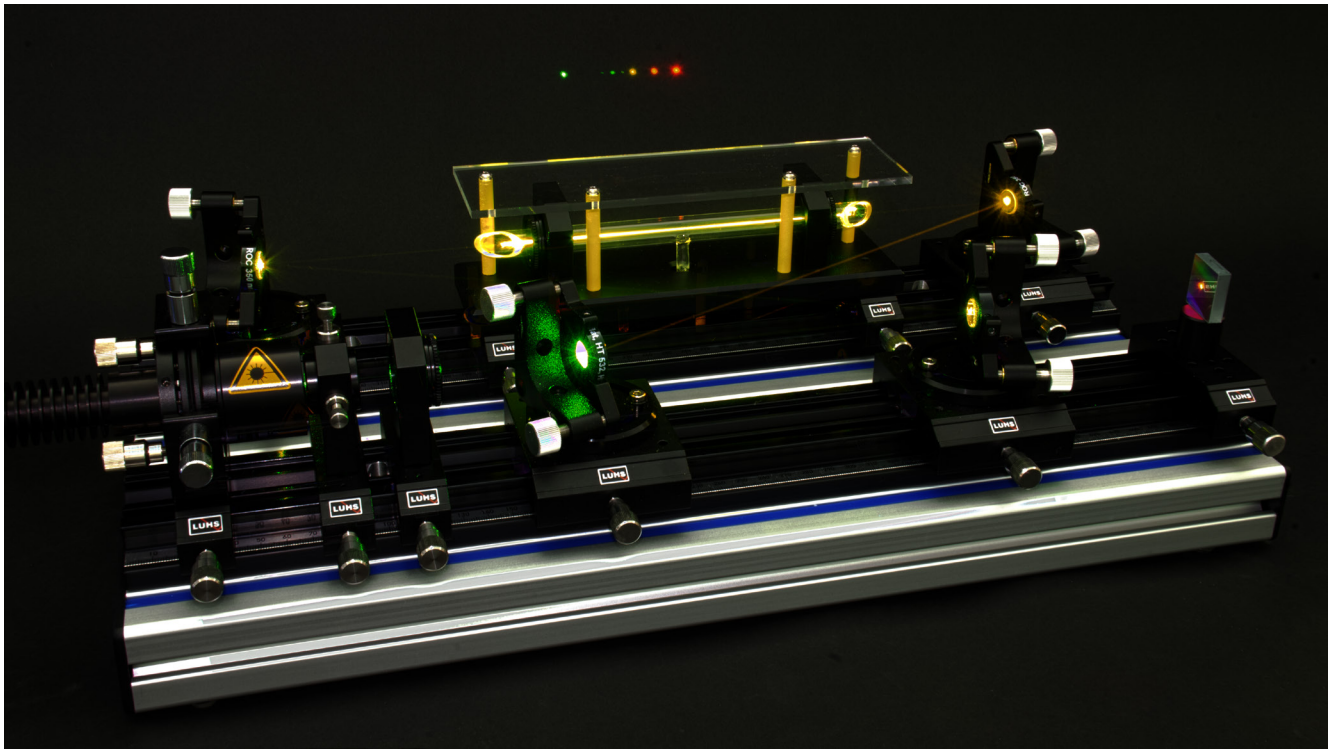

Table of Contents

1.0 Fundamentals

"The concept of a molecule as a combination of atoms emerged relatively late in scientific literature, at some time during the first half of the 19th century. One reason for this is that a large number of experimental investigations was necessary to replace the historical ideas of the "four elements" water, air, earth and fire, and the later alchemistic concepts of elements like such as sulphur, mercury, and salt (Paracelsus, 1493-1541) with an atomistic model of matter. A major breakthrough for this model were the first critically evaluated quantitative experiments investigating the mass changes involved in combustion processes, published in 1772 by Lavoisier (1743-1794), who might be called the first modern chemist". ... "Molecular spectroscopy originated during the first half of the 19th century. For example, in 1834 D. Brewster (1781-1868) observed, after spectral dispersion with the aid of a prism, hundreds of absorption lines, extending over the complete visible spectrum like Fraunhofer lines, when he transmitted sunlight through dense NO_2 gas over a vessel with nitric acid [1]. This was astonishing to Brewster, because he did not understand why the yellowish-brown NO_2 gas should feature absorption lines in the blue. He predicted that a complete explanation of this phenomenon would provide work for many generations of researchers, and - as we know today - his prediction turned out to be correct." [2]

^{1}H																	^{2}He
^{3}Li	^{4}Be											^{5}B	^{6}C	^{7}N	^{8}O	^{9}F	^{10}Ne
^{11}Na	^{12}Mg											^{13}Al	^{14}Si	^{15}P	^{16}S	^{17}Cl	^{18}Ar
^{19}K	^{20}Ca	^{21}Sc	^{22}Ti	^{23}V	^{24}Cr	^{25}Mn	^{26}Fe	^{27}Co	^{28}Ni	^{29}Cu	^{30}Zn	^{31}Ga	^{32}Ge	^{33}As	^{34}Se	^{35}Br	^{36}Kr
^{37}Rb	^{38}Sr	^{39}Y	^{40}Zr	^{41}Nb	^{42}Mo	^{43}Tc	^{44}Ru	^{45}Rh	^{46}Pd	^{47}Ag	^{48}Cd	^{49}In	^{50}Sn	^{51}Sb	^{52}Te	^{53}I	^{54}Xe
^{55}Cs	^{56}Ba	57..71	^{72}Hf	^{73}Ta	^{74}W	^{75}Re	^{76}Os	^{77}Ir	^{78}Pt	^{79}Au	^{80}Hg	^{81}Tl	^{82}Pb	^{83}Bi	^{84}Po	^{85}At	^{86}Rn
^{87}Fr	^{88}Ra	89..103	^{104}Rf	^{105}Db	^{106}Sg	^{107}Bh	^{108}Hs	^{109}Mt	^{110}Ds	^{111}Rg	^{112}Cn	^{113}Uut	^{114}Fl	^{115}Uup	^{116}Lv	^{117}Uus	^{119}Uuo
		↓															
		^{57}La	^{58}Ce	^{59}Pr	^{60}Nd	^{61}Pm	^{62}Sm	^{63}Eu	^{64}Gd	^{65}Tb	^{66}Dy	^{67}Ho	^{68}Er	^{69}Tm	^{70}Yb	^{71}Lu	
		^{89}Ac	^{90}Th	^{91}Pa	^{92}U	^{93}Np	^{94}Pu	^{95}Am	^{96}Cm	^{97}Bk	^{98}Cf	^{99}Es	^{100}Fm	^{101}Md	^{102}No	^{103}Lr	

Table 1: Periodic table showing the elements ( ) that exist as homonuclear diatomic molecules under typical laboratory conditions.

As time progressed, many scientists contributed to illuminate the manifold of atoms and sorted the atoms according to their atomic number in the periodic table of elements. In chemistry a sheer countless number of compounds of atoms, forming molecules are known and of course one wants to understand, classify, and calculate the binding and energetic properties the molecules and the quantum mechanics must be applicable as it already has been applied for the atoms. The easiest way to start, was to select the simplest atom available, the hydrogen. It consists of one proton and just one electron. However, the hydrogen exists only as molecule H_2 in nature. In order to study the spectrum of hydrogen atoms the H_2 molecules must be separated into "in statu nascendi" atoms. This is done inside a discharge tube by applying a voltage of 5 kV

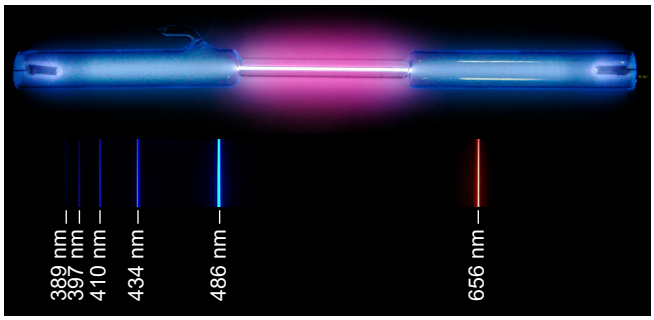

Fig. 1: Hydrogen atom visible spectrum (Balmer series) [3]

The Fig. 2 shows the energy level diagram of the hydrogen atom. The ground state has the ordering number *m=1* and the first excited state has *m=2*. To "lift" the electron into the first excited state requires an energy of about 10 eV, which is equivalent with a photon wavelength of 124 nm. This makes it clear, that a hydrogen atom or molecule respectively is not a good candidate for practical work, not to mention the potential explosive danger of hydrogen. However, due to its simplicity we will use it as example to understand the formation of molecules out of single atoms.

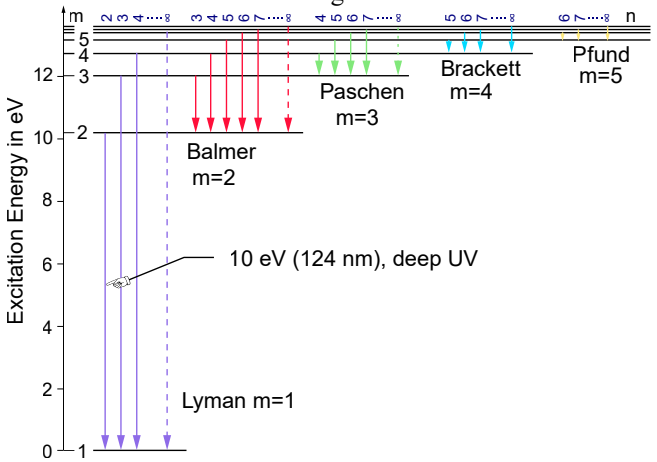

Fig. 2: Hydrogen atomic energy level diagram

Atoms at a large distance (compared to their spatial dimensions) to their neighbours can be considered as independent atoms and their energy levels are not influenced by the neighbouring atoms.

The behaviour will be different when the atoms are approached, as it is the case within a solid body. Depending on the type of atoms and their mutual interaction, the energy states of the electrons can change in a way that they even can abandon „their" nucleus and move nearly freely within the atomic structure. They are not completely free, otherwise they could leave the atomic structure.

How the „free" electrons behave and how they are organised will be the subject of the following considerations. From the fundamentals of electrostatics we know that unequal charges attract. Therefore it is easy to imagine that an atomic structure maybe formed by electrostatic forces. However, this model will fail when we try to justify the existence of solid Argon just by freezing it sufficiently. Since there is obviously

some sort of binding within the crystal structure, despite the fact, that the inert gases are neutral, there must be additional forces which are responsible for this sort of binding. To understand these forces, we must call on quantum mechanics for help. At the beginning this may be at bit difficult, but it simplifies the later understanding. The Hamilton operator and Schroedinger's equation are supposed to be known. We will briefly show the basic calculation to understand the formation of molecules at the example of hydrogen.

1.1 Binding of a hydrogen molecule

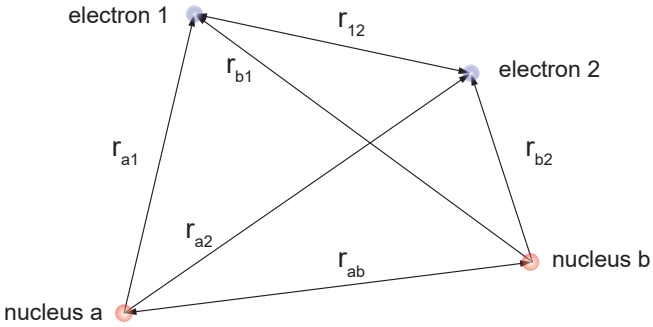

Fig. 3: Interaction of two hydrogen molecules

The total electric potential energy is:

$$U = -e^2 \cdot \left(\frac{1}{r_{a1}} + \frac{1}{r_{b2}} + \frac{1}{r_{b1}} + \frac{1}{r_{a2}} - \frac{1}{r_{ab}} \right) \qquad (1.1.1)$$

The following Schroedinger equation has to be solved:

$$\Delta\Psi_1 + \Delta\Psi_2 + 8\pi^2 \frac{m}{h^2} \cdot (E - U) \cdot \Psi = 0$$

For two hydrogen atoms without interaction the total energy will be

$$E = E_0(1) + E_0(2) = 2E_0$$

Correspondingly the eigenfunction ψ is the product of the eigenfunctions of the individual electrons belonging to the nuclei a and b.

$$\Psi_{12} = \Psi_a(1) \cdot \Psi_b(2)$$

Since we cannot distinguish between the individual electrons, the following linear combinations are valid eigenfunctions:

$$\Psi_{anti} = \Psi_a(1) \cdot \Psi_b(2) + \Psi_a(2) \cdot \Psi_b(1)$$
$$\Psi_{sym} = \Psi_a(1) \cdot \Psi_b(2) - \Psi_a(2) \cdot \Psi_b(1)$$

At the same time, Pauli's principle has to be respected, that means the eigenfunction Ψ_{ant} contains additionally the anti-parallel spins (↑↓ + ↑↓) and the function Ψ_{sym} the parallel spins (↑↑ - ↓↓). The electron distribution described by the linear combinations depends also on the distance dependent mutual electrostatic disturbance,

$$\Delta U = -e^2 \cdot \left(\frac{1}{r_{b1}} + \frac{1}{r_{a2}} - \frac{1}{r_{ab}} \right)$$

which are the reason for the mutual interaction. To get the complete solution, we have to add a „disturbance"-term to the undisturbed eigenfunctions Ψ_{ant} and Ψ_{sym}, as well as to the undisturbed energy. Then Schroedinger's equation becomes inhomogeneous because of the additional „disturbance" - term. As a solution we get:

$$E_{sym} = 2E_0 + e^2 \cdot C + e^2 \cdot A$$
$$E_{anti} = 2E_0 + e^2 \cdot C - e^2 \cdot A$$

We see that a term with the constant C representing the Coulomb part and a term with the constant A representing the interaction are added to the undisturbed energy. The exchange energy is based on the fact that electron 1 is localised near nucleus *a* at a particular instant and near nucleus *b* at another instant. The value of A can be positive or negative. The energy difference between the two possible energies is just

$$\Delta E = E_{sym} - E_{anti} = 2 \cdot e^2 \cdot A$$

A detailed calculation results in the following relation for C:

$$C = \int \left(\frac{1}{r_{ab}} - \frac{1}{r_{a2}} - \frac{1}{r_{b1}} + \frac{1}{r_{12}} \right) \cdot \Psi_a^2(1) \cdot \Psi_b^2(2) d^3r$$

and for A:

$$A = \int \left(\frac{1}{r_{ab}} - \frac{1}{r_{a2}} - \frac{1}{r_{b1}} + \frac{1}{r_{12}} \right) \cdot \Psi_a(1) \Psi_b(2) \Psi_a(2) \Psi_b(1) \cdot d^3r$$

Under respect of the fact that $\Psi_{a2}(1)$ and $\Psi_{b2}(2)$, integrated over the whole space represent probability densities which, multiplied by the elementary charge e, provide the total charge density ρ of the electrons 1 or 2 near the nuclei *a* or *b*, the constant C can also be written as:

$$e^2 C = \frac{e^2}{r_{ab}} - \int \frac{e^2 \rho_1}{r_{b1}} d^3r_1 - \int \frac{e^2 \rho_2}{r_{b2}} d^3r_2$$
$$+ \iint \frac{e^2 \rho_1 \rho_2}{r_{12}} d^3r_1 d^3r_2$$

We see that C results out of the attracting or repulsing Coulomb forces. The exchange integral A looks very much like the Coulomb integral. But the electron densities $\Psi_{2a}(1)$ resp. $\Psi_{2b}(2)$ have been replaced by the mixed terms $\Psi_a(1)$ $\Psi_b(2)$ and $\Psi_a(2)$ $\Psi_b(1)$ which are the result of the electron exchange.

Here we can summarise as follows: If atoms are mutually approached, the states of the undisturbed energy levels split into energetically different states. The number of newly created energy states corresponds to the number of exchangeable electrons (Fig. 4).

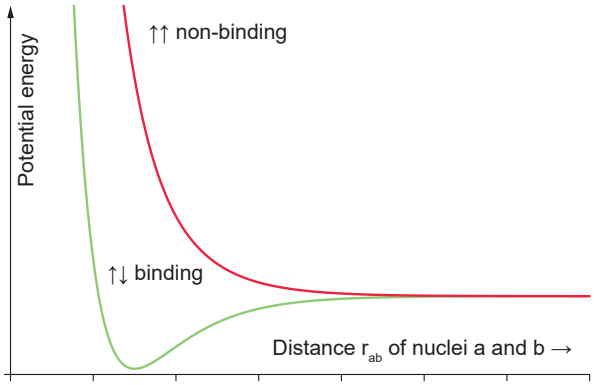

Fig. 4: Potential energy of two hydrogen atoms

One curve (↑↓) shows a minimum for a particular distance of the atoms. No doubt, without being forced the atoms will approach till they have acquired the minimum of potential energy. This is also the reason for hydrogen to occur always

as molecular hydrogen H_2 under normal conditions. The second curve (↑↑) does not have such a distinct property. The curves distinguish in so far as for the binding case the spins of the electrons are anti-parallel (↑↓). For the non-binding case they are parallel (↑↑).
It is easy to imagine that an increase of the number of atoms also increases the number of exchangeable electrons and in consequence also the number of newly generated energy levels. Finally the number of energy levels is so high and so dense that we can speak about an energy band. Here it is interesting to compare the action of the electrons with the behaviour of ambassadors.
The electrons in the most outside shell will learn first about the approach of an unknown atom. The eigenfunctions will overlap in a meaningful way. One electron will leave the nucleus tentatively to enter an orbit of the approaching atom. It may execute a few rotations and then return to its original nucleus.

If everything is OK and the spins of the other electrons have adapted appropriate orientations new visits are performed. Due to the visits of these „curious“ electrons the nuclei can continue their approach. This procedure continues until the nuclei have reached their minimum of acceptable distance. Meanwhile it cannot be distinguished which electron belongs to which nucleus.
If there is a great number of nuclei which have approached in this way there will also be a great number of electrons which are weakly bound to the nuclei. Still, there is one iron rule for the electrons: my energy level can only be shared by one electron with opposite spin (Pauli principle). Serious physicists may now warn to presume that there may be eventually male and female electrons, but who knows.....

Let’s return to incorruptible physics.

1.2 Molecule vibration and rotation

Now we understand how hydrogen atoms form molecules and in Fig. 5 real measured values are plotted..

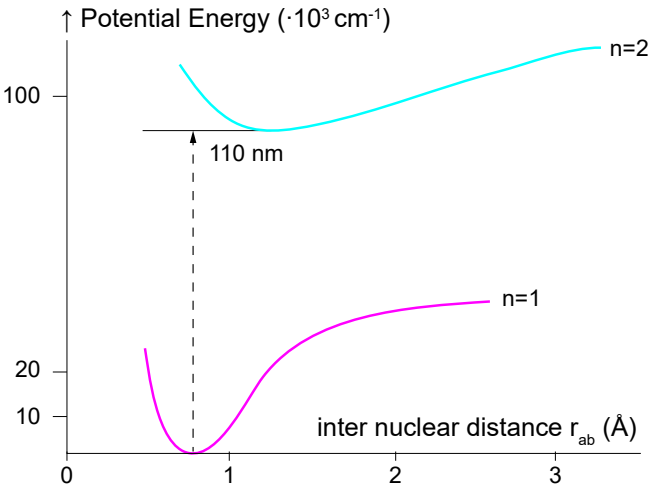

Fig. 5: Measured energy level diagram of H_2 molecules for the molecular ground (n=2) and first exited (n=2) state

The Fig. 5 shows two binding curves, one for two hydrogen atoms both in their electronic ground state forming a molecule. The upper curve shows the case when one of the hydrogen atoms was in the first exited electronic state when they decided to become a molecule.
Furthermore we notice that the minimum energetic distance between the first excited molecular state to the ground state is about 90.000 cm^{-1}. That means, we need a light source emitting radiation at a wavelength of 110 nm! Such laser exist, but they are extremely costly. Thus the researcher starts to search for a better suited atom, which also has just one electron in the outer shell, forming molecules, but having transition energies preferentially within the visible range. It turned out that Iodine was and is the best candidate.
In the following we will introduce a few more important properties at the example of a diatomic molecule, like the vibration and rotation energy level of such a molecule. Before the atoms form a molecule, they had no other degree freedom as translational movement. The spring like binding of the atoms results in additional degrees of freedom like vibration and rotation around the centre axis of the molecules. In a first approximation, we consider the molecule as two balls which are connected by an elastic spring as shown in Fig. 6.

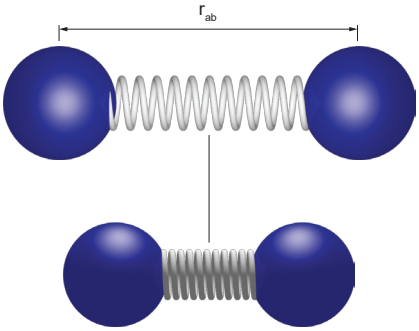

Fig. 6: Molecular vibration

We start with the classical analysis of the vibration of the molecule as a “body spring” system.

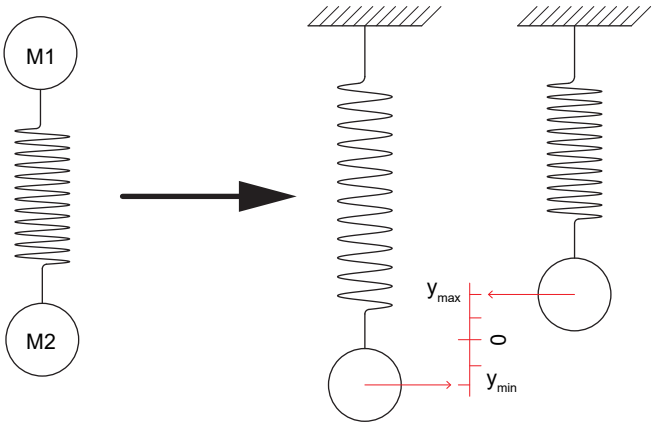

Fig. 7: Transform a two body to one body equivalent

The classical potential energy of a harmonic oscillator is given by:

$$V(y) = \frac{1}{2} \cdot k \cdot y^2$$

Whereby V(y) is the potential energy for a given value of the elongation y and k is the spring constant and ω is the oscillation frequency:

$$\omega = \sqrt{\frac{k}{m}}$$

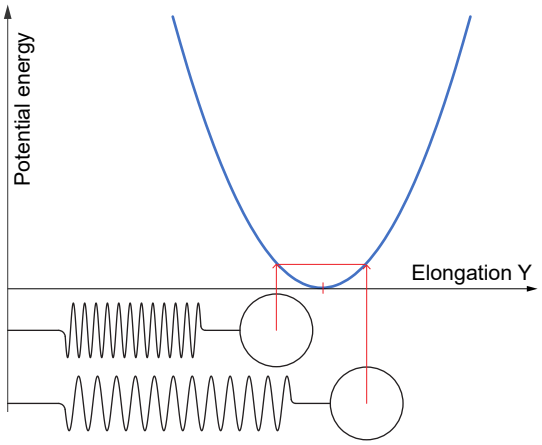

Fig. 8: Potential energy curve of the harmonic oscillator

We are now interested how the quantum mechanics treatment of the problem will look like. The non-relativistic Schrödinger equation for a single particle moving in an electric field is applied:

$$\left[-\frac{\hbar^2}{2\mu} \cdot \nabla^2 + V(r) \right] \Psi(r) = E(r)$$

We need to specify the potential energy V(r). For the harmonic oscillator, it is:

$$V(r) = \frac{1}{2} \cdot k \cdot r^2 = \frac{1}{2} \cdot m \cdot \omega^2 \cdot r^2$$

Instead of y, we introduced more general r as elongation,

$$\left[-\frac{\hbar^2}{2\mu} \cdot \nabla^2 + \frac{1}{2} \cdot m \cdot \omega^2 \cdot r^2 \right] \Psi(r) = E(r)$$

and solve the Schrödinger equation to obtain the eigenvalues of the energy.

$$E(v) = \left(v + \frac{1}{2}\right) \cdot \hbar \cdot \omega$$

First, the energy is quantized, meaning that only discrete energy values (v+½) multiples of $\hbar\omega$ are possible; this is a general feature of quantum-mechanical systems when a particle is confined. Second, these discrete energy levels are equally spaced. Third, the lowest achievable energy (the energy of the v = 0 state, called the ground state) is not equal to the minimum of the potential well, but $\hbar\omega/2$ above it; this is called zero-point energy. Because of the zero-point energy, the position and momentum of the oscillator in the ground state are not fixed (as they would be in a classical oscillator), but have a small range of variance, in accordance with the Heisenberg uncertainty principle. In some science fiction movies like "Stargate Atlantis" a so called ZPM (zero point modules) should be able to makes use of this energy. Next time you may watch such a movie, recall what you have learned here.

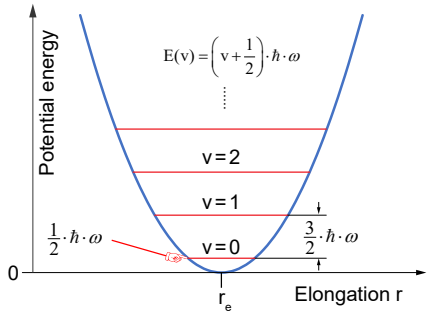

Fig. 9: Quantum harmonic oscillator

In the next step, we will analyse the classical energy based on the rotation of the molecule. We assume, that the rotation will not change the distance of both atoms, the molecule is considered as a rigid rotator.

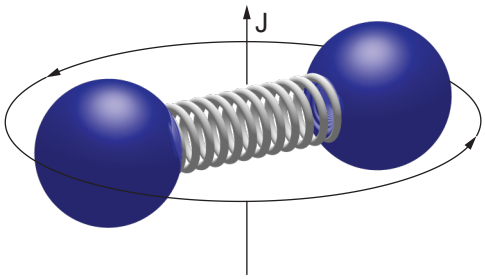

Fig. 10: Rotation of the molecule around its centre axis

Classical calculation yields the following expression:

$$E_{rot} = \frac{1}{2} \cdot J_x \cdot \omega^2$$

Jx stands for the moment of inertia and ω for the angular velocity.
The quantum mechanical treatment yields:

$$E_j = \frac{\hbar^2}{2 \cdot \mu \cdot r_{ab}^{\ 2}} \cdot j \cdot (j+1)$$

$$\mu = \frac{m_a \cdot m_b}{m_a + m_b}$$

$$E(j) = B \cdot J \cdot (J+1)$$

B is the abbreviation of the constant terms in front of the expression j(j+1) and is named as rotational constant.

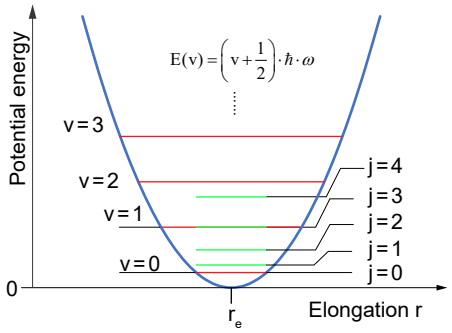

Fig. 11: Rovibronic energy level of a harmonic oscillator and rigid rotator

As already mentioned, the analysis so far is based on considerations of a harmonic system. Within the next approach, we need to find a way to modify the potential well of the harmonic oscillator to the real molecule.

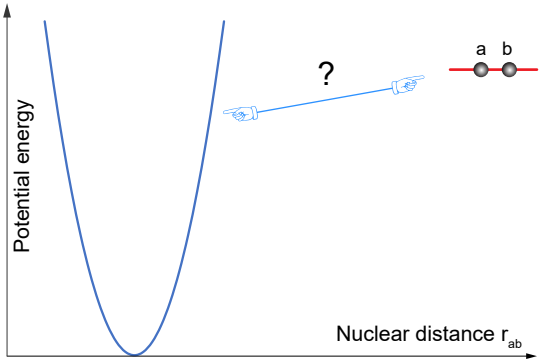

Fig. 12: Searching the link between the molecule and separated atoms

So far the results described the energy states within the harmonic well. However, they failed to interconnect to the situation of separated atoms. Meaning, that for providing enough energy the molecule should dissociate into single atoms again. Philip McCord Morse proposed 1929 a potential for a diatomic molecule. It is a better approximation for the vibrational structure of the molecule than the quantum harmonic oscillator because it includes the existence of unbound states.

$$V(r_{ab}) = D_e \cdot \left(1 - e^{-\alpha \cdot (r_{ab} - r_e)}\right)$$

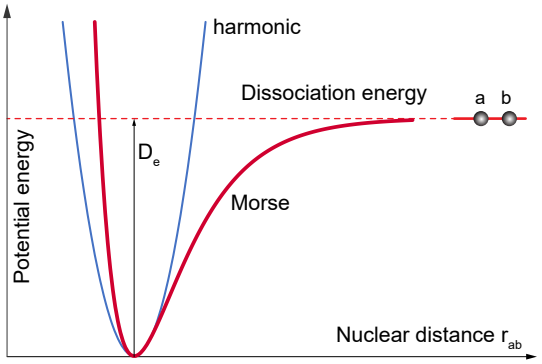

Fig. 13: Harmonic and Morse potential curves

Morse inserted his formula into the Schrödinger equation and obtained analytical solutions.

$$\left[-\frac{\hbar^2}{2\mu}\cdot\nabla^2+V_{Morse}(r)\right]\Psi(r)=E(r)$$

Comparing to the solution for the vibrational energy of the harmonic potential, an extra term occurs:

$$E(v)=h\cdot\nu_0\left(v+\frac{1}{2}\right)-\frac{h^2\cdot\nu_0^2}{4\cdot D_e^2}\cdot\left(v+\frac{1}{2}\right)^2$$

with

$$\nu_0=\frac{\alpha}{2\cdot\pi}\cdot\sqrt{\frac{2\cdot D_e}{\mu}}$$

The extra derivative is quadratic in the quantum vibration number v and reduces the energy distance for higher values of v (see Fig. 14). Especially near the dissociation limit, the distances become extremely small.

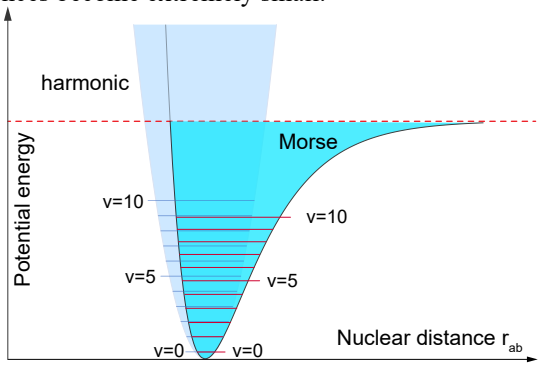

Fig. 14: Morse compared to harmonic potential

Although the Morse potential was a powerful approximation, however, as the experimental precision was increasing, deviations to the theoretical predicted potential became obvious. Thus, the experimentalists started to calculate the underlying potential based on their measurements. The accurate determination of potential curves for the different states of a molecule is among the major objectives of the spectroscopy of diatomic molecules.

Most of the precise potential curves have been derived from experimental data with the aid of different computational schemes. They rely on semi-empirical methods like the WKB procedure, an approximation method for the solution of the one-dimensional Schrödinger equation named after the initials of the inventors Wentzel, Kramers and Brillouin. It would be out of the frame of this introduction to explain the method, thus we refer to [2] for further details.

Finally we introduce the Dunham expansion which is a very common expression to calculate the rotational-vibrational energy levels of a diatomic molecule.

$$E_{vJ}=\sum_{j=0}^{\infty}\sum_{k=0}^{\infty}Y_{jk}\cdot\left(v+\frac{1}{2}\right)^j\cdot j^k\cdot(j+1)^k$$

Whereby v and j are the vibrational and rotational quantum numbers. The constant coefficients Y_{jk}, are called Dunham coefficients with $Y_{0,0}$ representing the electronic energy.

The Dunham expansion is valuable and practical tool to calculate and identify observed transitions inside molecular energy level.

1.3 Transitions between molecular energy levels

Up to now we have discussed possible energy levels of molecules. We will now discuss the properties of the homonuclear diatomic molecule I_2, used here, formed by identical iodine atoms.

There are many other homonuclear diatomic molecules as H_2, N_2, Na_2, Te_2, Se_2, but the iodine molecule is of specific importance and interest, as it has an absorption and emission spectrum covering the whole visible to near infrared spectral range with thousands of lines. Furthermore, it can easily be generated in sealed off cells containing solid iodine. The vapor pressure of solid iodine at room temperature is about 0.3 mbar and consists of I_2 molecules only.

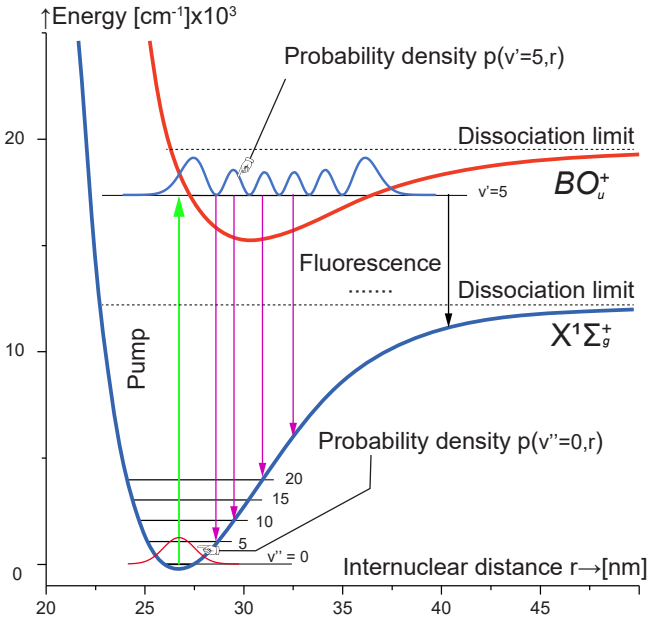

Fig. 15: Radiative transitions in a homonuclear diatomic molecule (dimer)

Fig. 15 shows a simple energy level diagram of I_2, consisting of the electronic ground state $X^1\Sigma_g^+$ and the first excited electronic state BO_u^+. Indicated are vibrational levels v'' = 0 up to v''= 20 in the electronic ground state and the vibrational level v' =5 in the excited electronic state (rotational levels are not shown). The vibrational levels will continue up to the dissociation limits, indicated by the dotted lines.

A specific feature of homonuclear diatomic molecules is that optical (dipole) transitions are only allowed between rotational-vibrational levels of different electronic states but not within one electronic state. A further selection rule for iodine is $\Delta J = \pm 1$ for the rotational levels, while for the vibrational levels all transitions with $\Delta v = 0, 1, \cdots n$ are possible. However, the strength of the transitions depends on the Franck-Condon coefficient q(v',v''), which are a measure for the overlap integral of the square of the vibrational wave functions *p(v,r)*, as shown in Fig. 15 for some vibrational levels. Especially favourable are therefore transitions which start from v''=0 (at the peak of the wave function) and end at the turning points for vibrational levels v' > 0 in the excited electronic state (Fig. 15). In addition, for the excitation of the molecule the population density in the rotational-vibrational levels of the electronic ground state is important, which is given by the Maxwell-Boltzmann distribution. This density is highest in the low lying levels (see Fig. 16) .

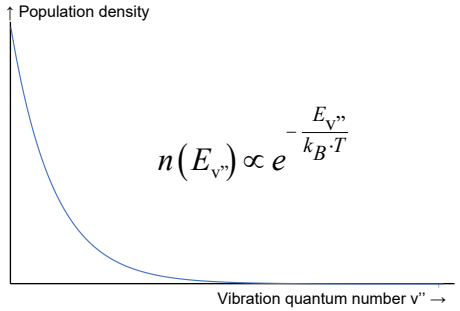

Fig. 16: Vibration Boltzmann distribution

Let us now consider the situation, when green laser light at 532 nm from the „laser pointer“ is directed into the iodine cell. The wavelength of 532 nm corresponds to an energy of 18797 cm^{-1}, which allows to shift the molecule from v''=0 of the electronic ground state to the vibrational level v'=32 in the excited electronic state, as shown in Fig. 17.

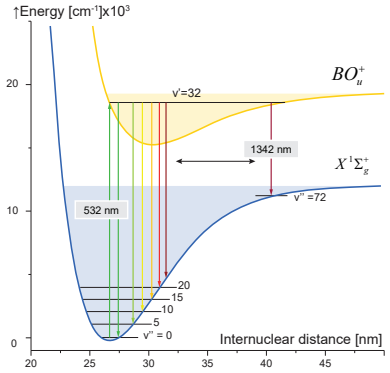

Fig. 17: Iodine excitation with a wavelength of 532 nm

After excitation, the molecules emit fluorescence lines, corresponding to transitions from the excited level v'= 32 to many vibrational levels of the electronic ground state, resulting in a fluorescence progression as measured in Fig. 18. The progression may extend up to v``= 72, far into the infrared, but ends here at v``= 35, due to the sensitivity limit of the used spectrometer. It should be noted, that the pump laser exactly excites the level v'=32, j'=57 in the excited electronic state, starting from v''=0, j''=56 in the electronic ground state. The fluorescence progression therefore consists of doublets with j''=56 and j''=58. However, these doublets are not resolved here by the spectrometer.

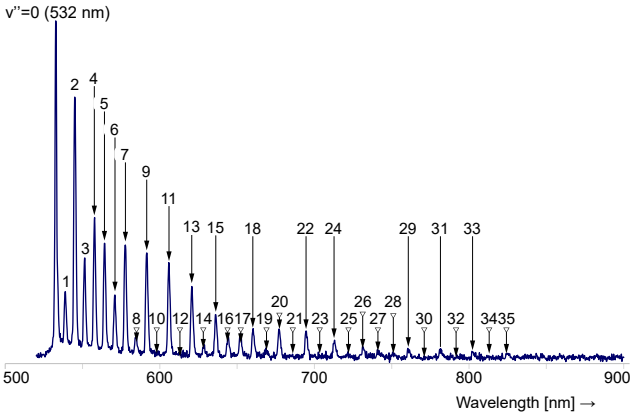

Fig. 18: Measured fluorescence spectrum

The question arises, how do we know or can determine the relevant vibrational number of the transitions? For this we have to look if there are lines on the shorter wavelength side of the pump line. These lines are called anti-Stokes lines. See also Fig. 19. If, for example, we would start from a level v''= 4 we would expect 4 anti-Stokes lines, terminating in levels v''= 3, 2, 1, 0. In the simple case as here, where we start from v``=0 we expect no anti-Stokes line, which is also shown by the spectrum. We can therefore simply index the peaks as done in Fig. 18.

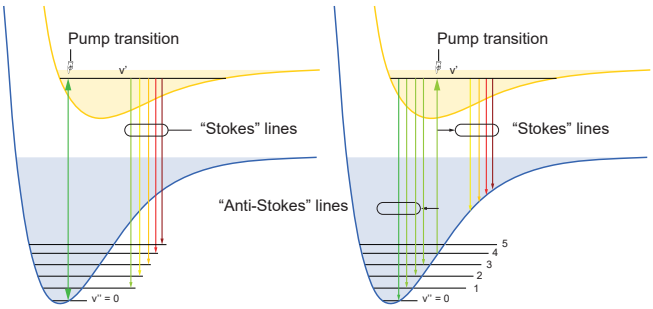

Fig. 19: Anti-Stokes and Stokes lines

From the progression data (vibrational numbers and transition wavelengths (energies) we may determine the Dunham expansion coefficients for the electronic ground state, according to the equation

$$E(v'') = Y_{00} + Y_{10}\left(v''+\frac{1}{2}\right) + Y_{20}\left(v''+\frac{1}{2}\right)^2 + Y_{30}\left(v''+\frac{1}{2}\right)^3 + \ldots$$

We ignore the rotational level in this simple approximation for the moment. The value for E(v'→v'') we take from the measured spectrum by converting the peak wavelength λ into energy in cm^{-1} using the relation $E(cm^{-1}) = 1 / \lambda(cm)$. The wavelength of 532 nm for instance is related to an energy of 18797 cm^{-1}.

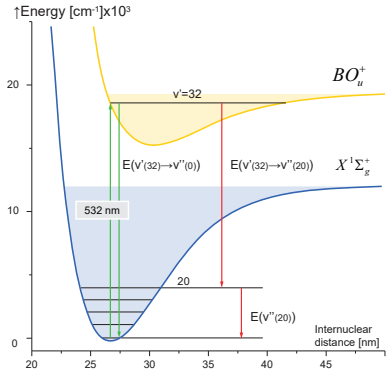

Fig. 20: Determine the energy E(v)

To determine the energy E(v'') from the measured spectrum, we need to calculate (see also Fig. 20):

$$E(v'') = E_{532nm} - E(v' \rightarrow v''),$$

with all energies given in cm^{-1} (1/λ). We may then create a plot of the energy values versus the vibrational number v'' given in Fig. 21.

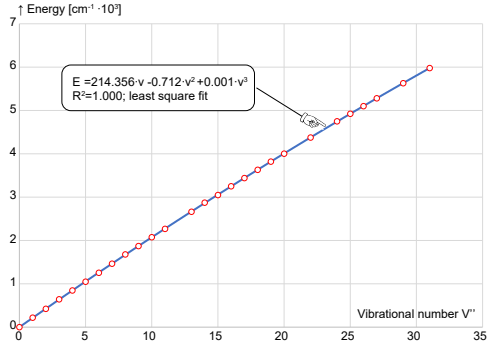

Fig. 21: Ground state Energy E(v'') for the Iodine molecule

A least square fit of the measured energies (wavelengths) yields good parameters for the Dunham expansion.

1.4 The iodine molecules as active laser material

In chapter 1.3 it has been shown, that by excitation of the iodine molecule with the "laser pointer" at 532 nm many fluorescence lines (Fig. 18) are obtained, covering a broad spectral range.

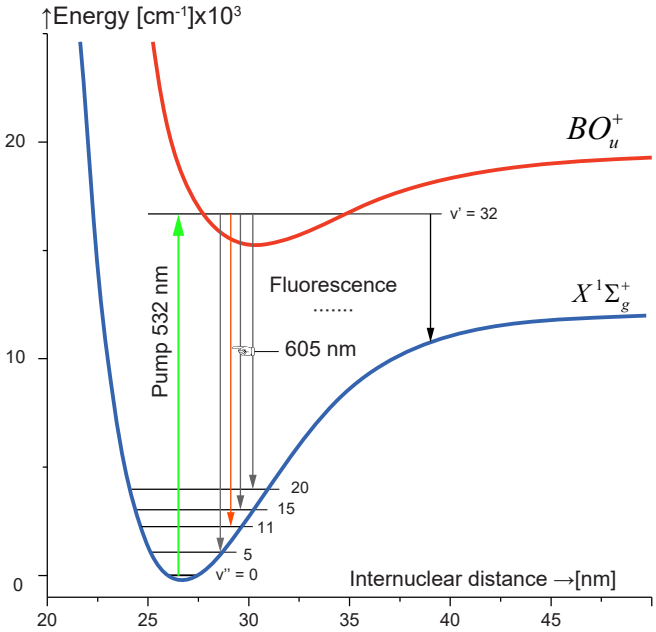

Fig. 22: Optical pumping of the iodine dimer

If the Iodine cell is now placed in a suitable optical resonator, cw laser oscillation on many of the fluorescence lines may be achieved. This was first reported by Wellegehausen et.al. [5] and independently by Koffend and Field [6].
In Fig. 22 a specific laser cycle with laser emission at 605 nm, corresponding to a transition v'=32 (BO_u^+) → v''=11 ($X^1\Sigma_g^+$) is shown. As can be seen, only 3 levels are involved in the laser cycle. This situation is shown again in the simplified energy level diagram of Fig. 23 where the involved levels are now named to E₁, E₂ and E₃. For simplicity, rotational quantum number have been omitted.

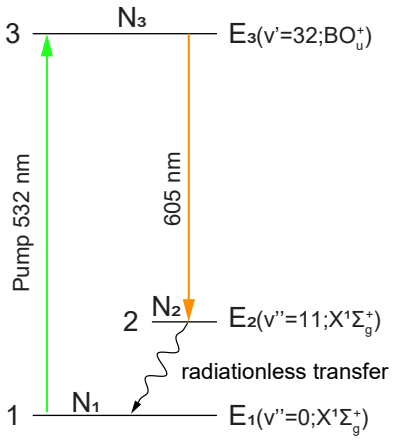

Fig. 23: Simplified energy level diagram

Considered as a normal laser, a necessary condition for laser oscillation is a population inversion N₃>N₂ between level 3 and 2. This can be achieved by a significant strong pump, if the relaxation between the levels 2 and 1 (radiationless transition) by collisions of the molecules is strong enough.
Typically, to achieve laser oscillation the iodine cell is placed into a ring resonator as shown in Fig. 24.

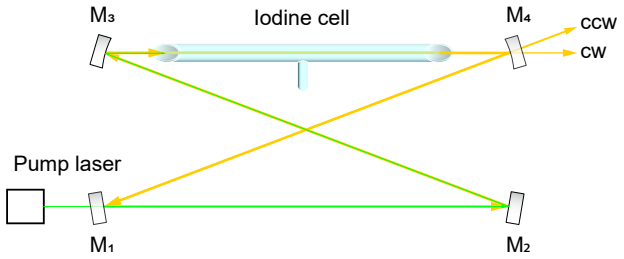

Fig. 24: Iodine ring laser

The beam of the pump laser is transmitted through the mirror M₁ and reflected by the mirror M₂ to the spherical mirror M₃, which creates a focus inside the iodine cell to increase the pump intensity. The mirror M₄ makes the beam parallel again and reflects it to the mirror M₁, which on his part reflects the beam to M₂ closing the round trip of the ring cavity.
Considered as a "normal laser", based on population inversion, one would expect now that in the ring resonator laser oscillation would occur in both directions with respect to the pump direction. Surprisingly, it does not, only unidirectional oscillation in direction of the pump laser occurs.
This behaviour has been observed for all cw dimer laser operated with Na_2, Te_2, Bi_2 and so on. Following the explanations as given in [4], this is due to the coherent coupling of the pump and laser radiation. Such coupling effects are well known and are the reason for the Raman scattering [7]. Whereas Raman observed and described the off resonant scattering (Fig. 25 A.), we are dealing here with a situation, where the pump wavelength and laser wavelengths are resonant to the absorption and emission transition of the molecule, corresponding to a resonant Raman scattering process (Fig. 25 B.).

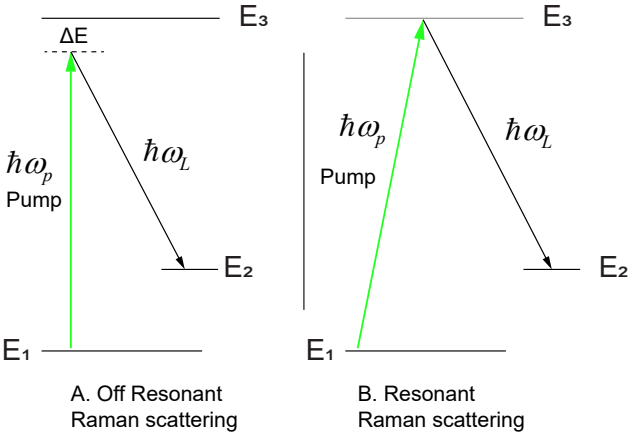

Fig. 25: Raman scattering

The Raman process is a two photon process, coupling two photons and performing a transition between the levels E₁ and E₂ with a more or less strong detuning $\Delta\omega=\Delta E/\hbar$ from resonance. This two photon process has to fullfil the resonance condition $\hbar\omega_p - \hbar\omega_L = E_2 - E_1$. Furthermore, to obtain Raman laser oscillation, the necessary condition for the population densities in the levels 1 and 2 is N₁>N₂, which is naturally fulfilled. A Raman laser process therefore needs no population inversion, as it is a coherent scattering process.
Let us now come back to the resonant process for iodine and the fact that we have a molecular iodine gas with moving molecules according to a Maxwell-Boltzmann velocity distribution. Assuming an independent absorption / emission

process (two step process), the situation is described by Fig. 26.

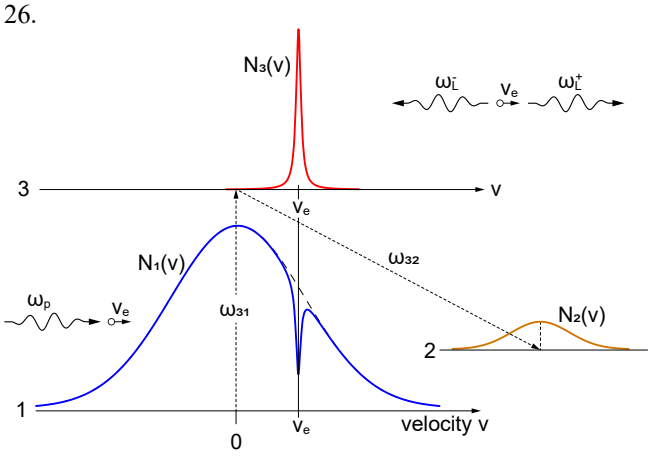

Fig. 26: Sub Doppler excitation-emission scheme

Pump radiation at frequency ω_p excites molecules around a velocity v_e and generates a narrow population distribution $N_3(v)$ in the level 3, from where the laser process may start. With $\omega_p = \omega_{31} + k_p \cdot v_e$ ($k_p = \omega_p/c$), laser emission from the excited molecules with velocity v_e is possible at frequencies:

$$\omega_L = \omega_{32} + \varepsilon \cdot k_L \cdot v_e$$

With ε=+1 for the forward and ε=-1 for the backward direction with respect to the pump direction.
Consequently the forward and backward frequencies are different, but for both cases the number of excited molecules participating to the amplification will be the same and no direction is preferred.
The situation changes, if we now consider a simultaneous absorption / emission (two photon process) which has to fulfil the resonance condition:

$$\omega_L^{\pm} = \omega_p - \frac{1}{\hbar}(E_2 - E_1)$$

Inserting the Doppler shifted frequencies for ω_{32} and ω_{31} we obtain:

$$\omega_L^{\pm} = \omega_p - \frac{1}{\hbar}(E_2 - E_1) + \left(1 - \varepsilon \frac{k_L}{k_p}\right) \cdot k_p \cdot v_e$$

$$\omega^{+} = \omega_p - \frac{1}{\hbar}(E_2 - E_1) + \left(1 - \frac{k_L}{k_p}\right) \cdot k_p \cdot v_e$$

$$\omega^{-} = \omega_p - \frac{1}{\hbar}(E_2 - E_1) + \left(1 + \frac{k_L}{k_p}\right) \cdot k_p \cdot v_e$$

For the two photon process all molecules may contribute, but due to the factor:

$$\left(1 - \varepsilon \cdot \frac{k_L}{k_p}\right) \approx 0$$

the forward frequencies ω_L^+ (ε = 1) are much less distributed than the backward frequencies ω_L^- (ε = -1), leading to a small and higher forward gain profile as compared to the backward direction as shown in Fig. 27.

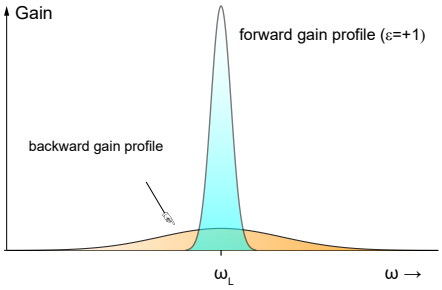

Fig. 27: Raman and inversion gain

Therefore, in general the forward direction is favoured. However, the coherent coupling process may be disturbed by collisions among the molecules or by collision with an additional buffer gas. Therefore also backward oscillation is possible and occasionally observed, but in general much weaker. For a more detailed discussion of the conditions for Raman gain or gain based on population inversion see [4].
A suitable resonator for the dimer lasers therefore is a ring resonator as shown in [Fig. 24].
Actually, it is a folded ring resonator also named as bow-tie ring resonator.

Fig. 28: This is a bow-tie

A bow-tie ring resonator geometry is often used to minimize astigmatism by keeping the incidence angles as small as possible.

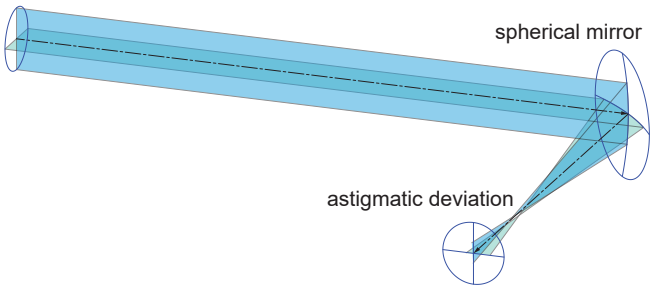

Fig. 29: Reflections at spherical mirrors causes astigmatic deviations

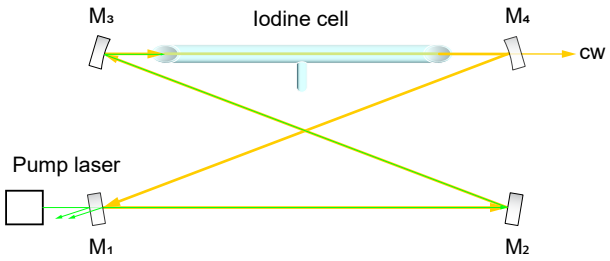

Fig. 30: Astigmatism compensated bow-tie ring resonator with unidirectional oscillation

If the ring resonator is symmetric and the radius of curvature of the mirror M_3 and M_4 are identical, the astigmatism is compensated. A further advantage of a ring cavity is, that the directions of the back reflected light from mirror M_1 and not absorbed pump power are different to the pump laser beam. Back scattered light into the pump laser may have detrimental effects on its mode stability.

1.5 Stability criterion of the four mirror bow-tie cavity

An optical resonator is considered as stable, if after an infinite number of beam reflections the beam is still smaller than the diameter of the mirror, otherwise the photons will leave the resonator. To determine if a resonator is stable the so called ABCD matrix formalism is applied. A general discussion of the ABCD matrix formalism can be found here [10] and especially for a 4 mirror ring laser the formalism is given here[10]. However, for a first information simple geometrical optical principles can be used.

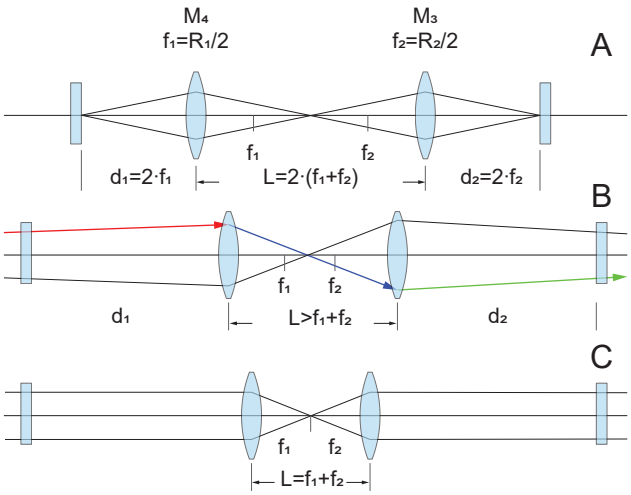

Fig. 31: Ring resonator as geometric optical structure

Apparently, the bow tie resonator is optically stable, when the distance L fulfils the following condition:

$$L \geq \frac{1}{2} R_1 + R_2 \qquad (1)$$

This case is shown in Fig. 31 (C). Since the beam propagating in the side arms d_1 and d_2 almost parallel, no requirements for the values of d_1 and d_2 needs to be fulfilled.

1.6 Line selection with a BFT

Birefringent crystals are indispensable in laser technology. They are used as optical retarder and also as tuning elements. At this point we will introduce a formalism describing the interaction between light and birefringent optics in a simple way. This formalism enables us to analyse and represent the way in which various birefringent components work, with regard to computer applications in particular.

1.6.1 Jones Matrix Formalism

Jones created the basis for this formalism in 1941. We should really be grateful to him. He was probably one of those people who didn't think much of exercises with complex numbers and sin and cos theorems.

The electric field intensity of light is usually represented in the vectorial form:

$$E = E_0 \cdot \sin(\omega t + kr + \delta)$$

E_0 is the amplitude unit vector describing the size and direction (polarisation) of the electrical field

$\omega = 2\pi\nu$, ν is the frequency of light
t is the time

$\vec{k}$ is the wave vector, containing the information of the propagation direction and the wavelength λ:

$\vec{r}$ is the displacement vector in the system of coordinates of the light wave

$$\delta = \frac{2\pi}{\lambda} \cdot |r_1 - r_2|$$

δ is a constant phase shift with respect either on a fixed coordinate or a fixed frequency

A complete description of a light wave still requires information on the magnetic field of the light wave. However, most of applications in optics with materials that do not absorb, the interaction of light is primarily of an electrical nature and not a magnetic one. As regard to strictly theoretical derivations the magnetic field must fulfil certain conditions for continuity at the boundary surfaces. We do not consider this aspect for the moment.

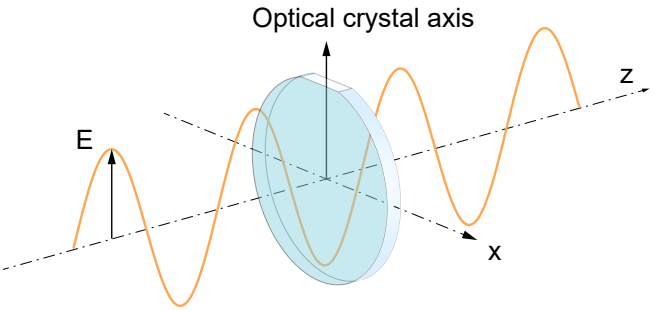

Fig. 32: Passage of a light wave through an optical plate.

The situation as shown in Fig. 32 is typical for the use of birefringent components. It is therefore sufficient to be interested only in the X and Y components of the electrical field E. Thus, the light wave will be described by:

$$J = \begin{pmatrix} E_x \cdot e^{i\omega t} \\ E_y \cdot e^{i\omega t + \delta} \end{pmatrix} \qquad (2)$$

Since the frequency of the X and Y amplitude will always be the same and for power calculations fast oscillating terms will be neglected, we can simplify (2) to:

$$J = \begin{pmatrix} E_x \\ E_y \cdot e^{i\delta} \end{pmatrix}$$

Let us normalise the power P of the light wave to 1. Then

$$P = E_x^2 + E_y^2 = 1$$

It can be deduced easily that:

$$P = J\, J^{-1}$$

The minus sign in the J exponent means the conjugate complex of J (substitute i by -i). For a light wave that is polarised in the direction of the Y-axis it will be:

$$J = \frac{1}{\sqrt{2}} \cdot \begin{pmatrix} 0 \\ 1 \end{pmatrix}$$

In an analogous representation for a wave polarised in the direction of X the equation would be:

$$J = \frac{1}{\sqrt{2}} \cdot \begin{pmatrix} 1 \\ 0 \end{pmatrix}$$

We know that, based on the validity of the superposition principle of linear optics, any given number of polarised linear waves can be represented by the vectorial addition of two mutually perpendicular individual waves. By adding the two Jones vectors given above we would get linear polarisation of light oscillating at 45 degrees to the X or Y axis.

$$J = J_1 + J_2 = \frac{1}{\sqrt{2}} \begin{pmatrix} 1 \\ 0 \end{pmatrix} + \frac{1}{\sqrt{2}} \begin{pmatrix} 0 \\ 1 \end{pmatrix} = \frac{1}{\sqrt{2}} \begin{pmatrix} 1 \\ 1 \end{pmatrix}$$

If one component has a phase shift δ with respect to the other component, the result will be elliptical polarised light. If the phase shift δ is λ/4 the result will be the circular polarisation of light.

$$\delta = \frac{2\pi}{\lambda} \cdot \Delta \quad , \quad \Delta = \frac{\lambda}{4} \Rightarrow \delta = \frac{\pi}{2}$$

The Jones vector for this kind of light has the following form.

$$J = \frac{1}{\sqrt{2}} \cdot \begin{pmatrix} 1 \\ i \end{pmatrix} \text{ note : } e^{\frac{i\pi}{2}} = i$$

An optical component, which can produce such a phase shift is called “birefringent” or double refractive. An element which works selectively on one component only works as polariser. The difference between the two is that whereas the polariser removes a component, the birefringent plate slows one component down to the other, in a way that the components differ in phase behind the plate. Before giving the Jones matrices for these elements we will explain briefly the way the elements work.

A simple model will be used for this purpose. Light will be observed as an electromagnetic oscillation. We consider the optical component as a collection of many dipoles. The dipole of the atom or molecule depends on the type and form of the electron shells. The electromagnetic field of the light excites the dipoles and are thus turned out of their equilibrium (susceptibility). The dipoles absorb energy of the light (virtual absorption) and transmit them out again. However, a dipole cannot transmit its radiation in the direction of its own axis.

If a crystal has two kind of dipoles, which are at a particular angle to one another, they can only emit and absorb light within the area of their angles. If the process of absorption and emission is slower in one kind of dipole than in the other there will be a phase shift. Macroscopically it seems as if there were a higher refractive index. A change in beam direction takes place because of the different dipole directions, i.e. there are two separate beam directions within the component. If a parallel light beam penetrates into this kind of material the result is, indeed, two beams leaving the crystal and both beams are polarised perpendicularly and have a phase shift between each other.

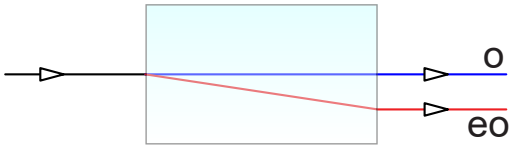

Fig. 33: Birefringent crystal

This phenomenon is called birefringence. These two marked directions of the crystal also have two distinctive refractive indices. Since one beam appears to be violating the Snell’s law, it is called extraordinary (eo) and the one behaving normally is ordinary (o). Crystalline quartz and calcite are materials which behave in this way. There are also a series of other crystals but these two proved successful in laser technology. Thin plates, used as optical retarder are mostly made out of quartz because it is hard enough for this purpose.

Mica sheets have also been used but they are not suitable for use inside the resonator because of the losses involved. Please note that only crystalline quartz has a birefringent behaviour. Quartz that has already been melted (quartz glass) loses this property. A whole series of laser components are made out of calcite [8]. Short calcite crystals are sufficient to produce the required beam separation, e.g. as with the active Q-switch, because of the great difference between the ordinary and extraordinary refractive indices.

The Jones matrix formalism is a mathematical description of the interaction of a light wave with such materials. Retarding plates and polariser can be represented as Jones matrices in the same way that a plane wave can be represented as a Jones vector. Polariser which allow polarised light to pass in x or y are given as follows:

$$P_x = \begin{pmatrix} 1 & 0 \\ 0 & 0 \end{pmatrix} \text{ and } P_y = \begin{pmatrix} 0 & 0 \\ 0 & 1 \end{pmatrix}$$

If the polariser is turned around the beam over the angle θ, P must be treated with the transformation or rotational matrix:

$$R(\theta) = \begin{pmatrix} \cos(\theta) & \sin(\theta) \\ -\sin(\theta) & \cos(\theta) \end{pmatrix}$$

and the result for the turned polariser will be:

$$P(\theta) = R(-\theta) \cdot P \cdot R(\theta)$$

A birefringent plate, whose optical axis is parallel to the x or y axis, has the following Jones matrix:

$$V = \begin{pmatrix} e^{-i\frac{\delta}{2}} & 0 \\ 0 & e^{i\frac{\delta}{2}} \end{pmatrix}$$

and needs to be transformed by the rotational matrix R(θ) if the optical axis of the crystal was rotated around the angle θ. To prevent misunderstandings regarding the optical axes, we must point out that the optical axis of the crystal is the one in which the ordinary refractive index is effective.

A birefringent plate made out of crystal quartz is used in the Iodine experimental laser for selecting single wavelengths. This kind of element is also known as a birefringent filter or birefringent tuner (BFT). This element was originally used to tune dye lasers. It was first successfully used in a He-Ne laser [9]. The arrangement within the laser cavity is shown in Fig. 34.

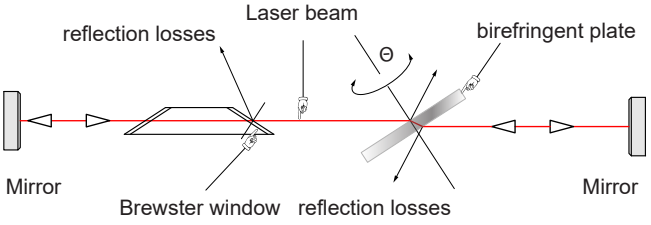

Fig. 34: Birefringent filter for wavelength selection inside the resonator

The birefringent plate is placed under the Brewster's angle into the resonator of laser to avoid reflection losses through the plate itself. The laser oscillates only in a direction of the polarisation given by the Brewster's window. The birefringent plate does not change the polarisation if a phase shift of $\delta = 2\,\pi$ occurs between the ordinary and extraordinary beam after passing through it twice. In this case there will be no reflection losses at any component which is oriented under the Brewster's angle. The polarisation of the returning wave changes at every other value of the phase shift δ and causes significant reflection losses at the Brewster's windows and prevent laser oscillation.
We are now interested in calculating the phase shift δ caused by the rotation of the plate. We start with the optical path of the ordinary beam:

$$l_o = d \cdot n_o ,$$

and the path of the extraordinary beam is

$$l_{eo} = d \cdot n_{eo} .$$

$$l_o - l_{eo} = d \cdot \left(n_o - n_{eo}\right)$$

the phase shift δ is :

$$\delta(\theta) = \frac{2\pi}{\lambda} \cdot 2 \cdot d \cdot \left(n_o - n_{eo}(\theta)\right)$$

The light travels twice the geometric path d. The plate has a thickness of D and θ is the angle between the electric field vector of light and the optical axis of the crystal lying in the plane of the plate. If the equation below is fulfilled,

$$\delta(\theta) = \frac{2\pi}{\lambda} \cdot 2 \cdot d \cdot \left(n_o - n_{eo}(\theta)\right) = 2\pi$$

then there are no losses at the Brewster's window. This applies to a given wavelength for a particular angle θ. Now, the thickness D and the rotational angle θ of a plate must be determined using the Jones matrix formalism and which fulfil the above condition in the wavelength area of visible lines of the Iodine laser.

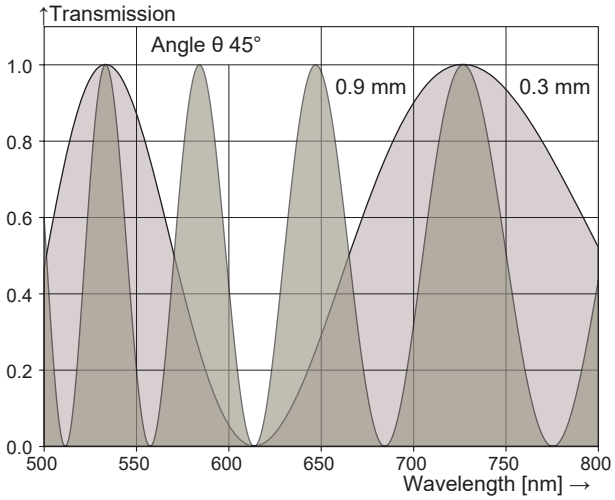

Fig. 35: Transmission of a BFT

Fig. 35 shows the transmission of a plate with a thickness of 0.9 and 0.3 mm, an angle of 45° between the electrical field vector and the optical axis calculated for a wavelength range of 500 - 800 nm. The dispersion of the crystalline quartz (Fig. 36) leads to a broadening of the transmission curve for higher wavelength. By turning the plate (changing angle Θ) the curves are shifted and the transmission peaks are located at different wavelengths. A BFT with a single plate has periodic transmission peaks which allows the simultaneous oscillation on several wavelengths, if they are within the laser gain range.

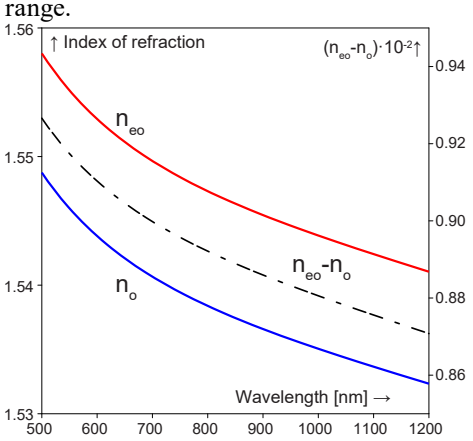

Fig. 36: Dispersion curve for the ordinary and extraordinary refractive index of crystalline quartz

1.7 Hyperfine structure

The nuclear spin of the Iodine atom is ≠ 0 resulting in an interaction of the nuclear spin with the electron shell and causes the splitting of energetic levels. In the Iodine molecule the influence of the other atom needs to be considered as well. An introduction to the theory of the hyperfine structure of diatomic molecules can be found in [12] and especially for Iodine molecule is given in [13] . We are concerned with the detection and analysis of such hyper fine structures, using the oscillation of the Iodine ring laser itself. For this purpose the Iodine ring laser is equipped with a BFT to ensure the stable operation of just one selected line and a PZT for changing the cavity length (Fig. 37).

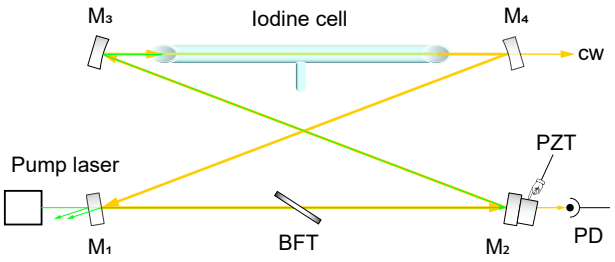

Fig. 37: Setup to observe and measure hyperfine laser lines

PZT is the abbreviation for lead zirconate titanate (**Pb**[**Zr**$_{(x)}$ **Ti**$_{(1-x)}$]O_3 ($0 \le x \le 1$)) and is one of the world's most widely used piezoelectric ceramic materials. If an electric field is applied to a piezoelectric material, deformation occurs in what is known as the inverse piezoelectric effect. PZT for optical applications are integrated into a housing which is designed in such a way that the PZT is preloaded for best linearity. Low voltage PZTs consist out of a stack of elements so that a translation of 1µm/10V is achieved. At a voltage of 150 V a translation of 15 µm can be achieved. A core hole allows the transmission of the light beam through the PZT. The PZT is connected to its controller to generate the scanning ramp voltage and the photodetector is connected to an oscilloscope.

As the Iodine laser is pumped with a single frequency pump laser, it will oscillate in a single frequency only (as long as there are no transversal modes). For optimum oscillation at a wavelength λ, the cavity has to be resonant, which for a ring cavity of length L means $L=n\cdot\lambda$, with n being an integer. o tune the cavity from one to the next resonance, a length shift of λ is required. For a wavelength of 600 nm this is equivalent to 0.6µm. Therefore we need to apply a voltage shift of 6V to achieve the tuning from one to the other resonance.

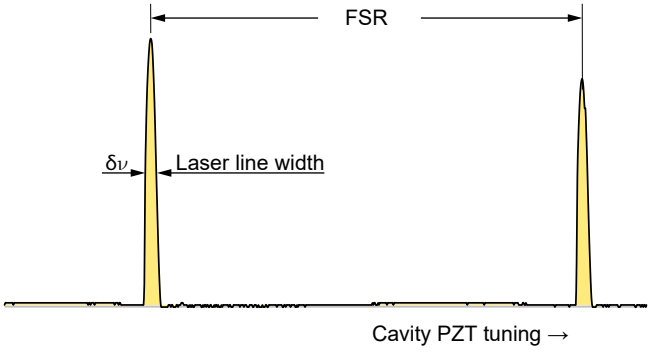

Fig. 38: Measured Laser power profile

Such a tuning is shown in (Fig. 38). The signal of the photodetector PD (Fig. 37) is displayed on an oscilloscope while the PZT is periodically scanned. The free spectral range is calculated by the relation $FSR=c/L$ and provides a calibration factor for the time axis of the oscilloscope in Hz. For a resonator length of about L=1.43 m, the FSR is about 210 MHz. The measurement indicates a single line with a narrow profile as expected. For some laser lines however, a more complex structure is obtained as shown in Fig. 39. This is due to the above mentioned hyperfine splitting and shows lasing on hyperfine components.

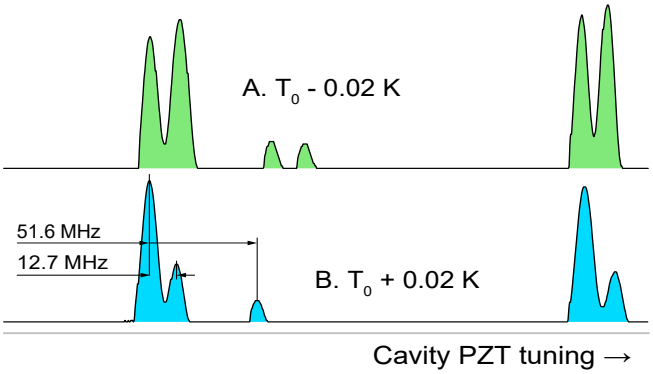

Fig. 39: Power profiles of hyperfine laser lines

The Fig. 39 shows two measurements A and B, they differ in the temperature (wavelength) of the pump laser. A and B are detuned by 0.04 K to each other, which means a detuning of 178 MHz (4.45 GHz/K) of the pump laser.

2.0 Description of the components

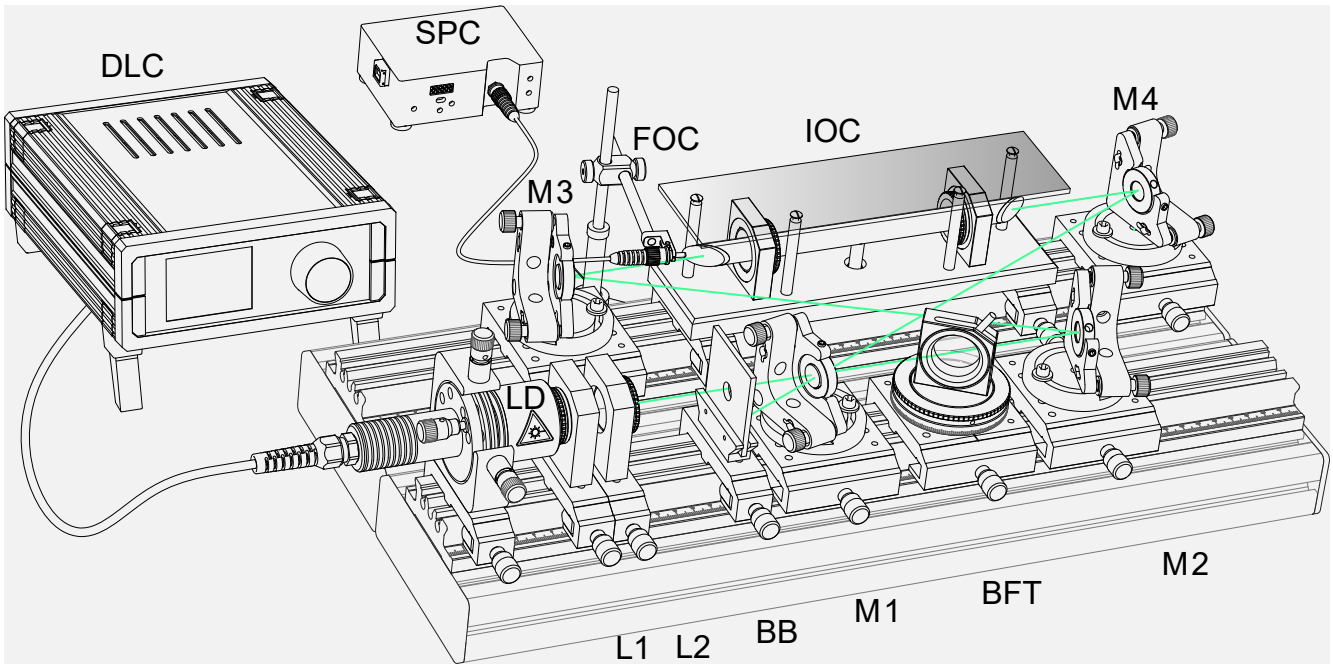

Fig. 40: System overview

The Laser Source (LD)

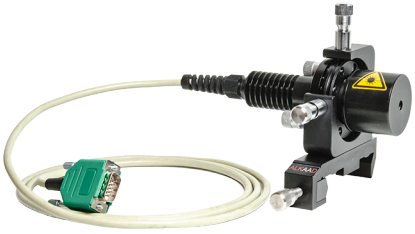

Fig. 41: Temperature stabilized LD

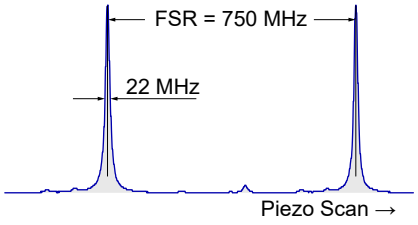

Fig. 42: Fabry Perot scan of the LD

The green Laser Module (GLM) is mounted inside the housing between two Peltier elements. After connecting with the digital controller, the temperature can be set in a range from 10 to 35°C and is kept constant within 0.01°C. The line width of the GLM is less than 22 MHz, which can be proved by using the "LM-0300 Fabry Perot Spectral Analyser". The maximum output power at 532 nm is 40 mW single mode and can be adjusted to a desired or recommended level.

2.7.1 Digital Diode Laser Controller

The laser diode module is connected via the 15 pin HD SubD jacket (LD). The controller reads the EEPROM of the laser diode and sets the required parameter accordingly. The MK1 is powered by an external 12V/ 1.5 A wall plug supply. A USB bus allows the connection to a computer for remote control. Furthermore firmware updates can be applied simply by using the same USB bus.

The MK1 provides an internal modulator which allows the periodic switch on and off of the diode laser. A buffered synchronisation signal is available via the BNC jacket (MOD). Furthermore the duty cycle of the modulation signal can be varied in a range of 1...100 % to enable the measurement of thermal sensitivity of the optically pumped laser crystal.

The controller is equipped with industrial highly integrated circuits for the bipolar Peltier cooler (Maxim, MAX 1978) as well as for the injection current and modulation control (iC Haus, iC-HG) of the attached laser diode. Further detailed specifications are given in the following section of the operation software.

Fig. 1: Digital Diode Laser Controller MK1

2.7.2 Diode laser controller screens

When the external 12 V is applied, the controller starts displaying the screen as shown in the figure below.

Fig. 2: Start screen

Laser Safety

The first interactive screen requires the log in to the device since due to laser safety regulations unauthorized operation must be prevented. In general this is accomplished by using a mechanical key switch. However, this microprocessor operated device provides a better protection by requesting the entry of a PIN.

After entering the proper key the next screen is displayed and the system is ready for operation.

Fig. 3: Authentication screen

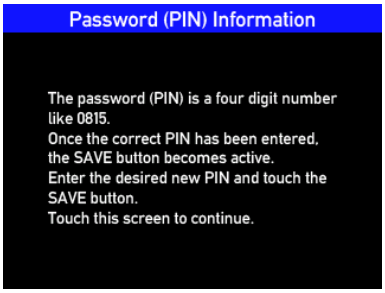

Fig. 4: Information for the password

Main Screen

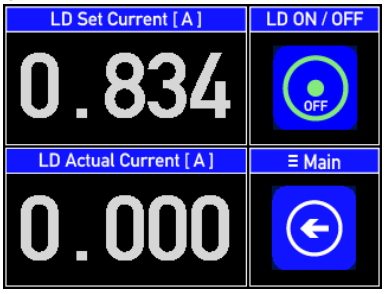

For immediate “Laser OFF” just tap the yellow button. To set the injection current simply tap the injection current display and turn the settings button (SET).

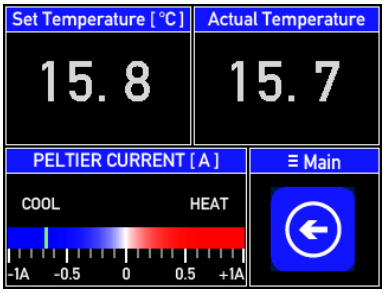

The same is true also for the “Set Temperature” section. When in operation and connected to the laser diode the actual temperature is shown in the “Actual Temperature °C section. Furthermore the actual current of the Peltier element is shown in such a way, that cooling or heating of the element can be observed.

Information screen

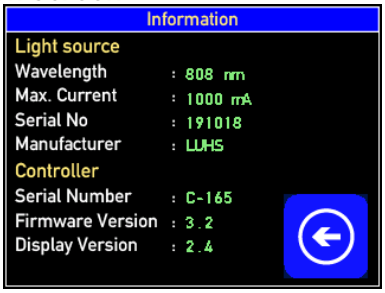

When tapping the Device Info button of the main screen this screen comes up. It again reads and displays the information stored in the EEPROM of the attached diode laser. If an entry exceeds the maximum or minimum limit value retrieved from the EEPROM of the attached diode laser the entry is reversed to the respective minimum or maximum value.

Modulation settings

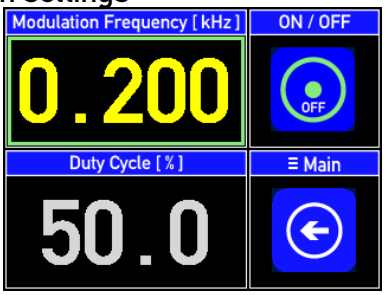

The diode laser can be switched periodically on and off. This is for a couple of experiments of interest. By tapping the display of the modulation frequency the entry is activated. Turning the settings knob will set the desired frequency value. The modulation becomes active, when the Modulator ON/OFF button is tapped.

Duty Cycle settings

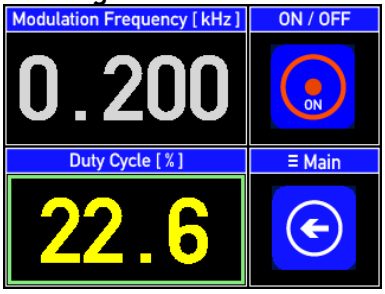

For some experiments it is important to keep the thermal load on the optically pumped laser crystal as low as possible or to simulate a flash lamp like pumping. For this reason the duty cycle of the injection current modulation can be changed in a range of 1...100 %. A duty cycle of 50% means

that the OFF and ON period has the same length. The set duty cycle is applied instantly to the injection current controller.

Overheating warning

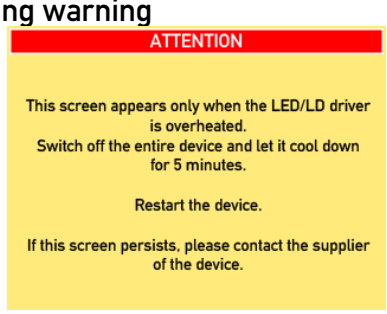

This screen you should never see. It appears only when the chip of the injection current controller is over heated.
Switch of the device, wait a couple of minutes and try again.
If the error persists please contact your nearest dealer.

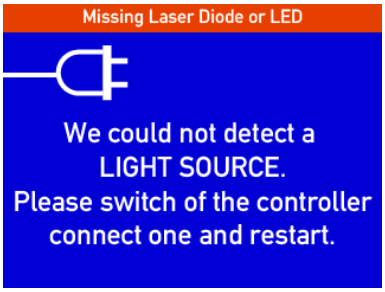

This screen is self explanatory and appears either when no laser diode is connected or the data reading from the EEPROM is erroneous.

Module LE1

The diameter of the green pump radiation emitted by the diode laser is very small and thus strongly divergent and needs to be collimated and made parallel. This is done by a combination of a concave lens L1 having a focal length of -15 mm. A plan-convex lens with a focal length of 50 mm is mounted into a C25 mount with a free opening of 20 mm. The mounted lenses are placed into the mounting plates, where they are kept in position by three spring loaded steel balls.

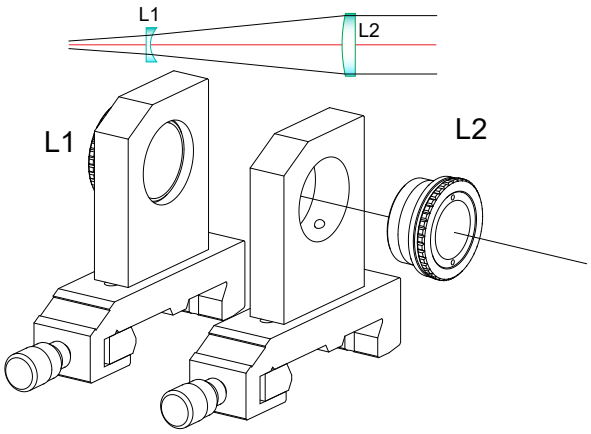

Ring laser mirror mount M1 (Fig. 40)

A kinematic mirror adjustment holder is mounted to a turn table in such a way that the front surface of the attached laser mirror lies always within the centre of the rotation axis. The turn-table is placed on top of a 65 mm wide carrier. Once the desired position has been set, the turn-table is fastened by means of a M4 fixing screw. This version is assembled for the lower left mirror of a ring laser structure. The corresponding laser mirror is set into an adapter with an outer diameter of 1" which fits into the kinematic laser mirror adjustment mounts. The mirror is kept in position by a radial grub screw with a soft nylon tip. The laser mirror has a flat surface and a high reflectivity (>99.9%) in a wavelength range of 550 to 800 nm and a high transmission for 532 nm.

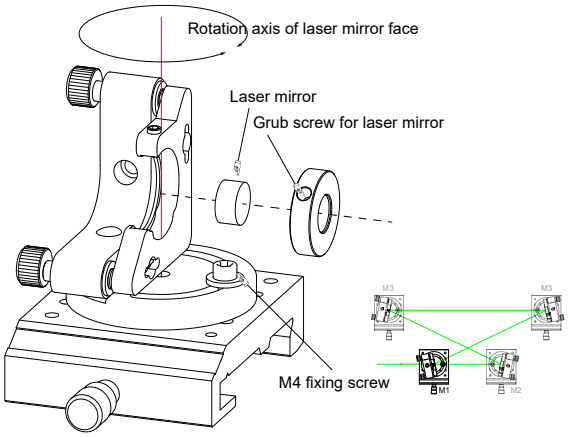

Ring laser mirror mount M2

A kinematic mirror adjustment holder is mounted to a turn table in such a way that the front surface of the attached laser mirror lies always within the centre of the rotation axis. The turn-table is placed on top of a 65 mm wide carrier. Once the desired position has been set, the turn-table is clamped by means of a M4 fixing screw. This version is assembled for the lower right mirror of a ring laser structure. The corresponding laser mirror is set into an adapter with an outer diameter of 1" which fits into the kinematic laser mirror adjustment mounts. The mirror is kept in position by a radial grub screw with a soft nylon tip. The laser mirror has a flat surface and a high reflectivity (>99.9%) in a wavelength range of 500 to 800 nm.

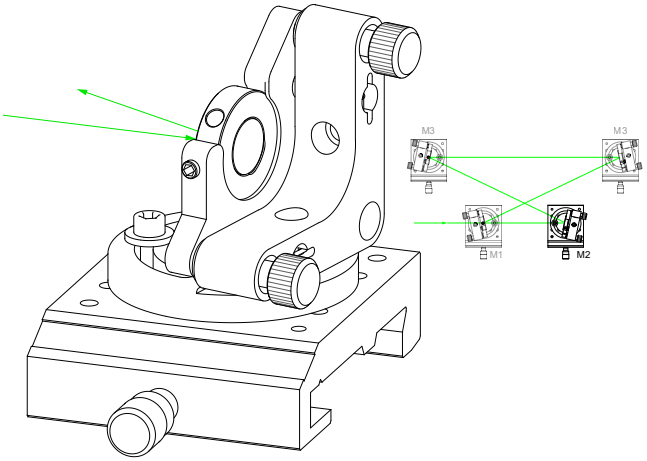

Ring laser mirror mount M3

A kinematic mirror adjustment holder is mounted to a turn table in such a way that the front surface of the attached laser mirror lies always within the centre of the rotation axis. The turn-table is placed on top of a 65 mm wide carrier. Once the desired position has been set, the turn-table is clamped by means of a M4 fixing screw. This version is assembled for the upper left mirror of a ring laser structure. The corresponding laser mirror is set into an adapter with an outer diameter of 1" which fits into the kinematic laser mirror adjustment mounts. The mirror is kept in position by a radial grub screw with a soft nylon tip. This laser mirror has a radius of curvature of 350 mm and a high reflectivity (>99.9%) in a wavelength range of 500 to 800 nm

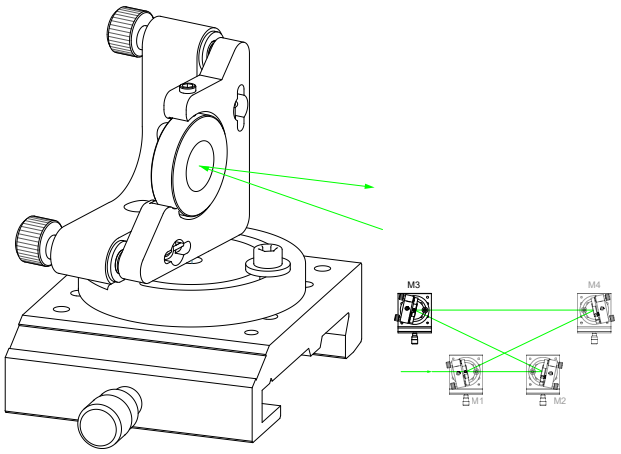

Ring laser mirror mount M4

A kinematic mirror adjustment holder is mounted to a turn table in such a way that the front surface of the attached laser mirror lies always within the centre of the rotation axis. The turn-table is placed on top of a 65 mm wide carrier. Once the desired position has been set, the turn-table is clamped by means of a M4 fixing screw. This version is assembled for the upper right mirror of a ring laser structure. The corresponding laser mirror is set into an adapter with an outer diameter of 1" which fits into the kinematic laser mirror adjustment mounts. The mirror is kept in position by a radial grub screw with a soft nylon tip. This laser mirror has a radius of curvature of 350 mm and a high reflectivity (>99.9%) in a wavelength range of 500 to 800 nm

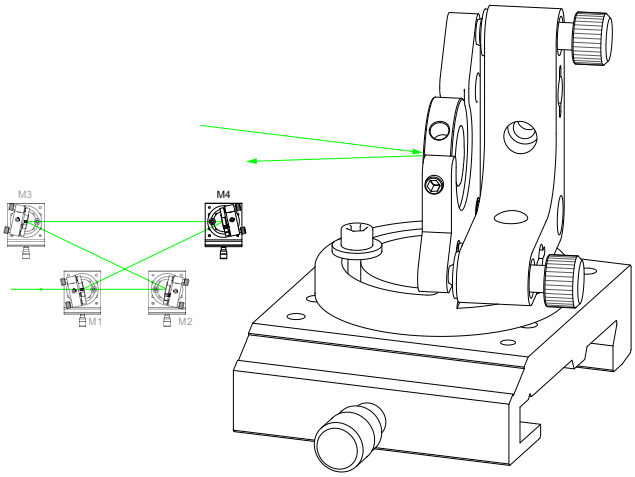

Iodine cell on carrier (IOC)

The glass cell has a length of 200 mm and Brewster windows at each side. It is baked out at a high temperature and natural Iodine is distilled into the evacuated cell and subsequently sealed. The cell is kept with soft rubber rings inside the two C25 mounts which are placed into two mounting plates. A plexiglass cover protects the valuable cell against damage.

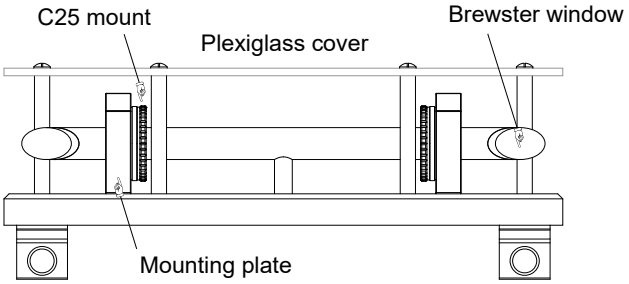

Birefringent Tuner (BFT)

The double refractive or birefringent plate (P) is mounted into a dual rotational stage. For the intra-cavity operation the birefringent plate needs to be aligned in such a way that the laser beam hits the plate under the Brewster angle to minimize the reflection losses by turning the rotary plate (B). In addition the birefringent plate can be rotated around its optical axis by tilting the lever (L). By rotating the plate its optical retardation δ is changed. If the retardation δ of two passes is a multiple integer of the wavelength λ the polarisation remains unchanged. In all other cases the polarisation is changed and will cause losses at the Brewster windows.

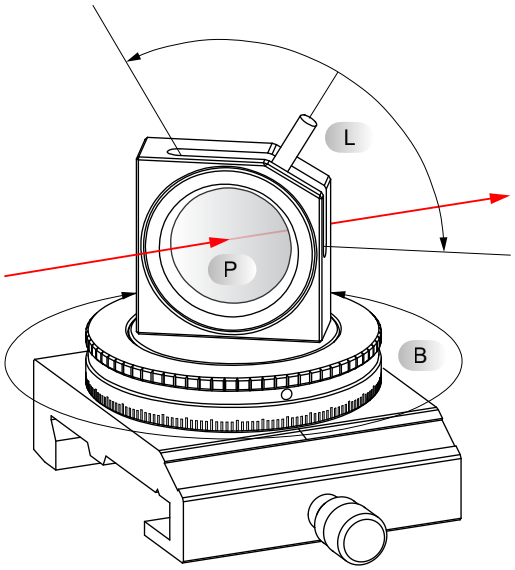

3.0 Experiment Setup

3.1 Iodine Spectroscopy

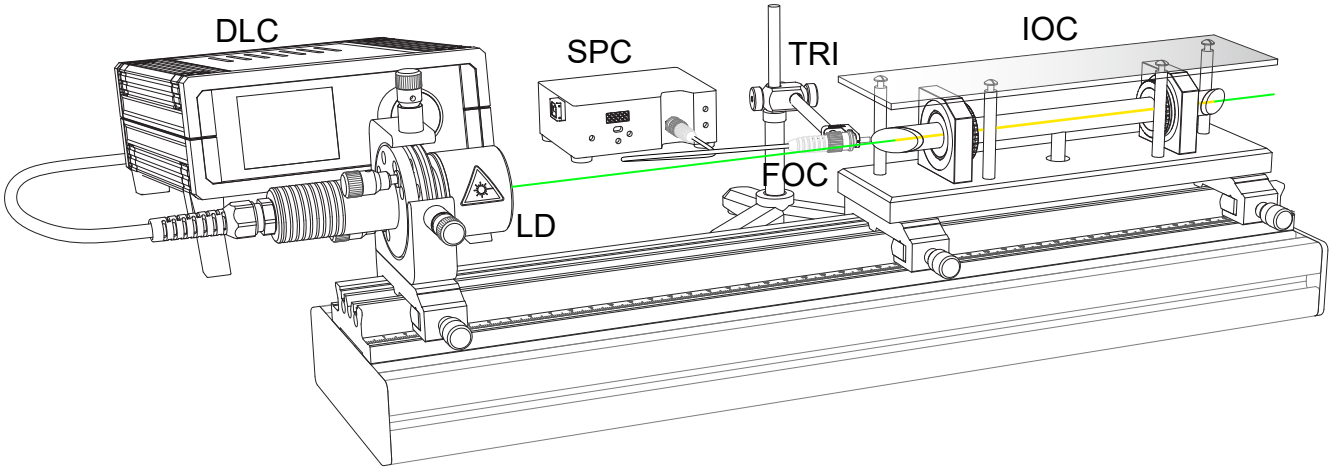

For this experiment we need only one rail. The laser (LD) is placed to the utmost left of the rail. The iodine cell (IOC) is placed to the utmost right position. The holder (TRI) holds the glass fibre ferrule and is positioned in such a way, that it looks in direction of the fluorescence track. The position is aligned for maximum fluorescence signal. At the beginning of the experiment the power of the pump laser (LD) is set to its maximum (350 mA), which is related to an output power of 40 mW. The temperature is set for maximum fluorescence, however, this temperature cannot be predicted and must be found for each experiment. Within a temperature range of typically 28-30°C the best absorption and strongest fluorescence will be found. Once fluorescence comes up, turn the knob by 3 retention ticks in one direction and observe if the fluorescence becomes stronger or weaker. Within 15-20 minutes the temperature for best absorption should be found.

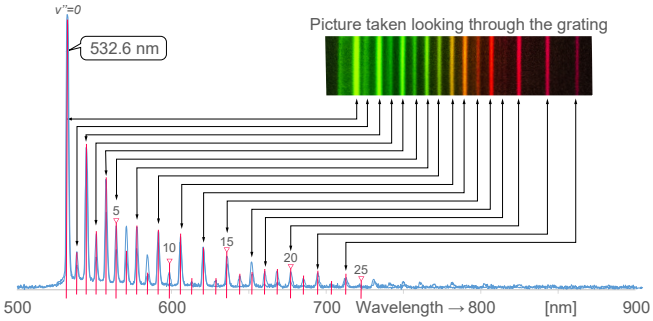

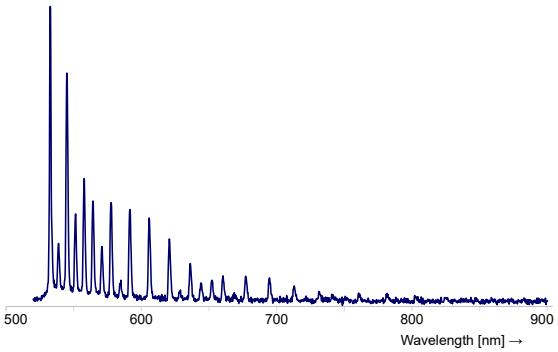

Fig. 1: Fluorescence spectrum

On the computer display a spectrum as shown above will be recorded and needs to be interpreted. If a spectrometer is not available, the spectrum can be taken by using the provided grating. The grating is held in front of the lens of a digital camera while taking a picture.

3.2 Ring Laser Setup

3.3 Step 1: Align the pump laser

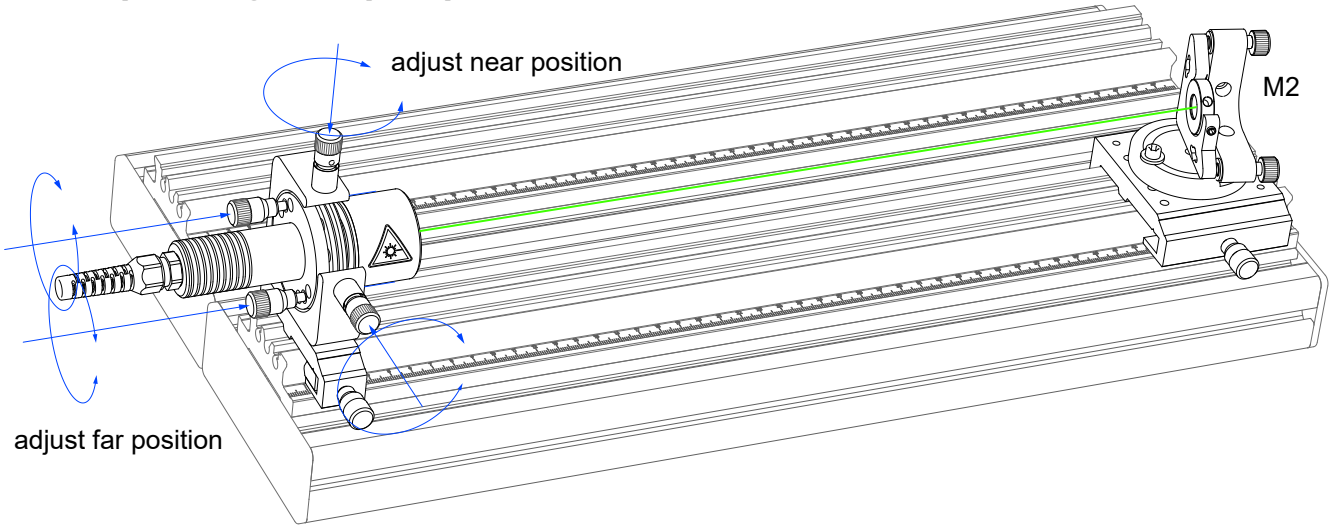

Place the laser in the utmost left position and the mirror M2 to the utmost right position onto the rail. By using the two fine pitch adjustment screws (far position, only one is visible) align the beam to the centre of the mirror M2. Move the mirror M2 close to the laser and align to the centre of the mirror M2 by using the other two fine pitch screws. Repeat the step until there is no change of the position of the laser spot on the mirror M2 in the near and far position.

3.4 Step 2: Place Mirror M1 and M2

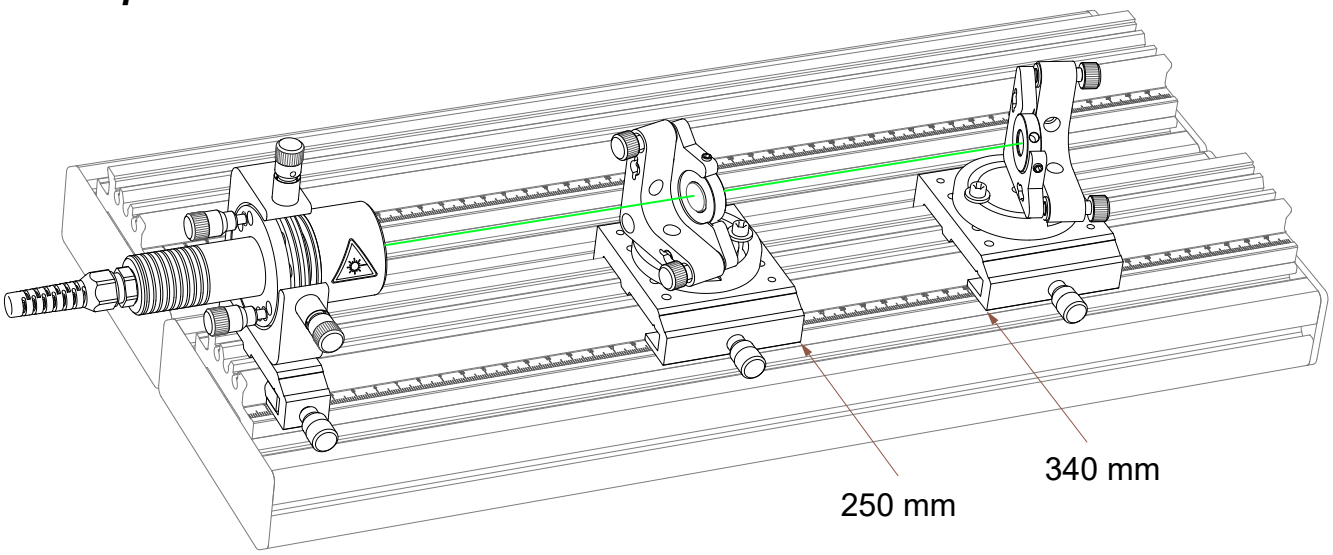

Place in addition to mirror M2 the mirror M1 onto the rail. The location should be as shown in the figure above. The positions are read from the ruler.

3.5 Step 3: Place the Iodine Cell and the Mirror M3

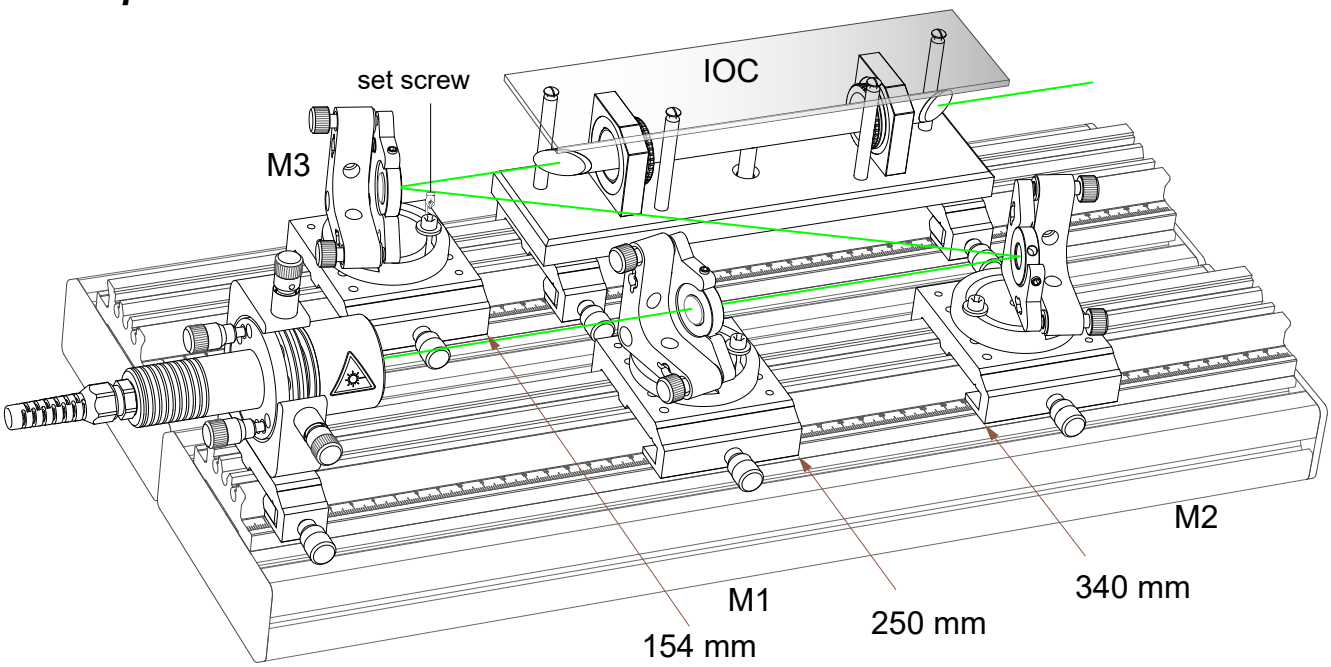

Place the iodine cell in the middle of the second rail. Set the Mirror M3 onto the second rail at the position 154 mm as shown in the figure above. The carrier of the mirror has a width of 65 mm and the centre of the mirror is at 32.5 mm. The stability criterion of the ring laser requires a distance between mirror M3 and M4 of slightly larger than 350 mm. The rail has a length of 500 mm. From these values the position of M3 and M4 can be calculated. It is good praxis to set M3 at 154 mm.

Fix the carrier of M1, M2 and M3 in its position. Place the beam collimator LE1 between the laser and the mirror M1. In the next step the beam hitting the mirror M2 is aligned in such a way, that the beam hits the centre of the mirror M3. For the coarse alignment, the set screw is slightly loosened with the provided Allan key (2.5 mm). Mirror M2 is gently turned until the beam hits the mirror M3. The set screw is fastened again and the fine alignment is done with the fine pitch adjustment screws of mirror M2.

3.6 Step 4: Align mirror M2

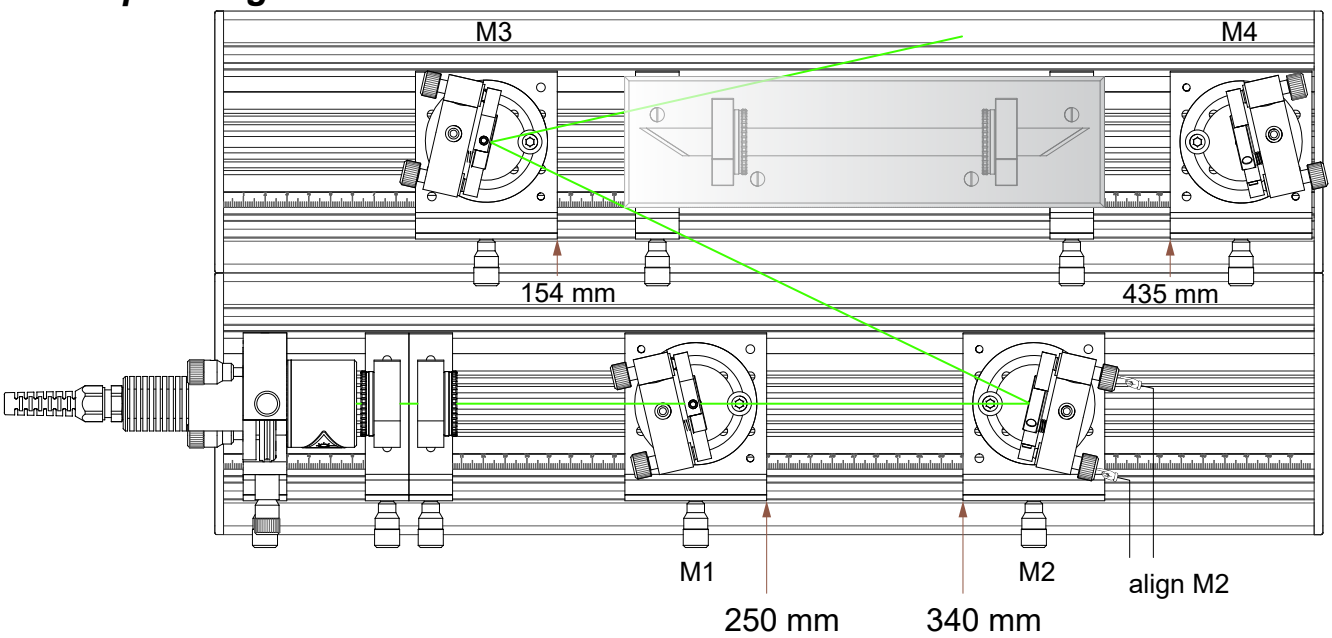

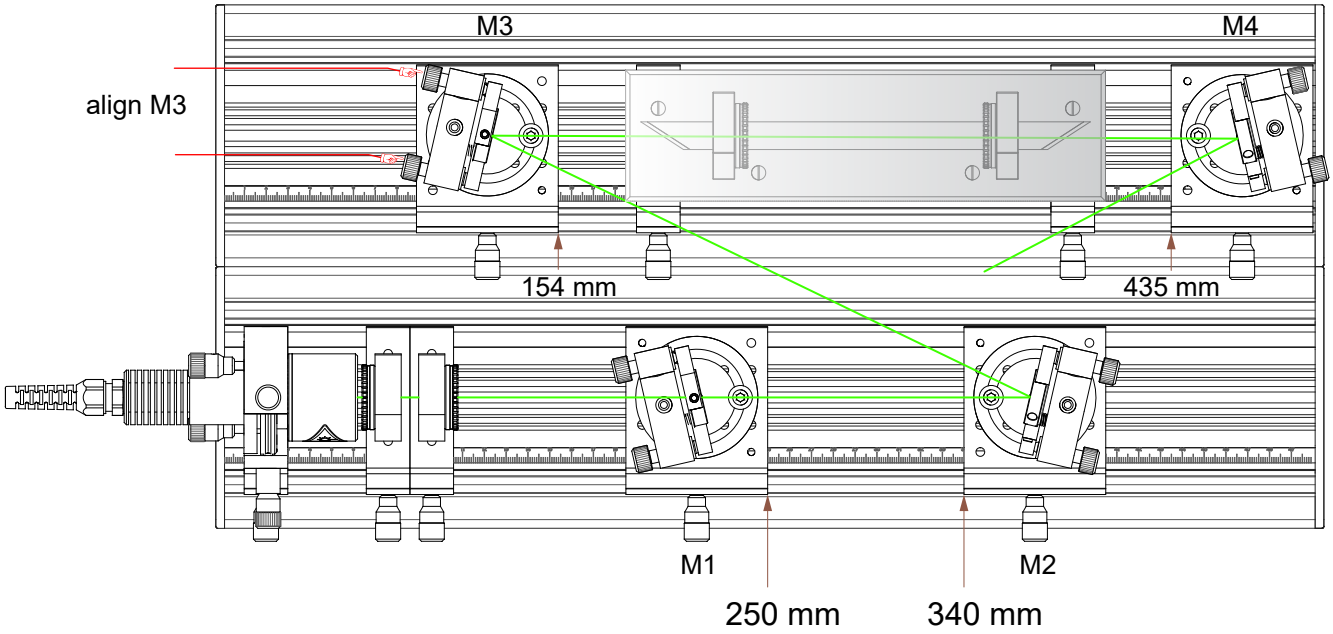

Adjust the mirror M3 such, that the beam passes the iodine cell and hits the mirror M4 in its centre. If required, make use of the coarse alignment as already mentioned.

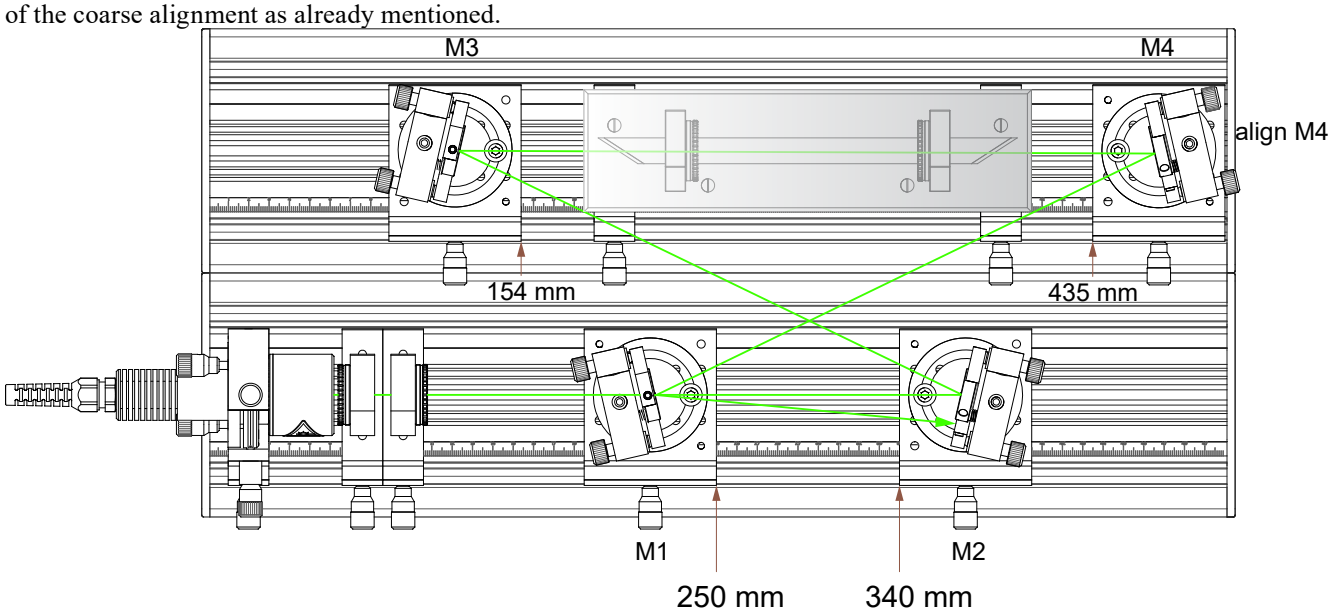

Once the beam hits the mirror M4 perfectly in its centre, the beam is aligned to the mirror M2 exactly to the spot where the incoming beam passes the mirror M1.

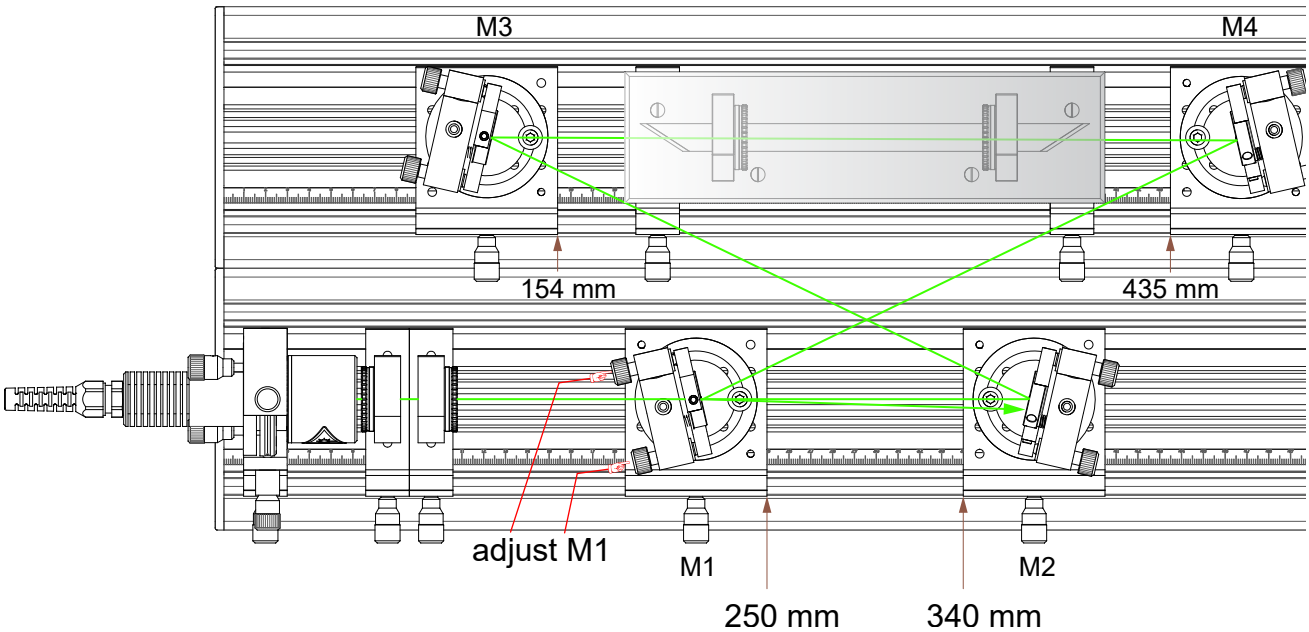

In the final step the reflected beam from M1 is aligned to hit the spot of the incoming beam on the mirror M2. Now the beam path of the ring laser is closed. The intensity of the reflex from mirror M1 may be weak and the alignment should be done in a darkened room.

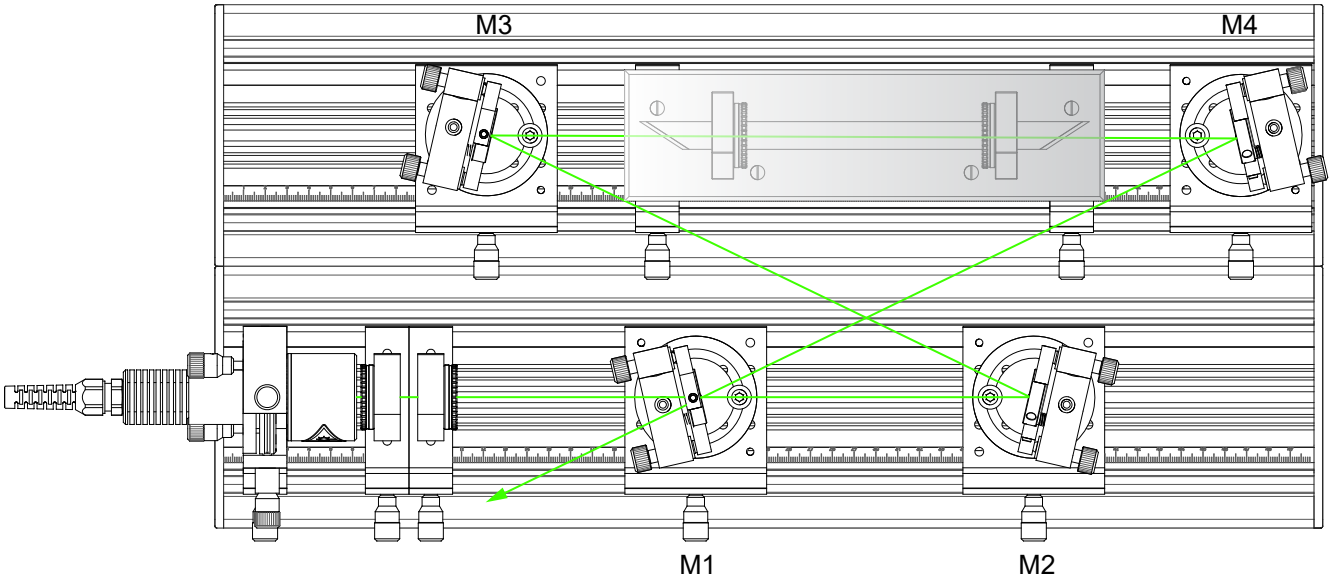

The ring laser is aligned! It must be noted that the mirror M1 has a high transmission for the pump radiation of 532 nm. Thus the non absorbed pump light which comes from M4 will be transmitted at M1. To avoid safety risks, we place the beam blocker into position.

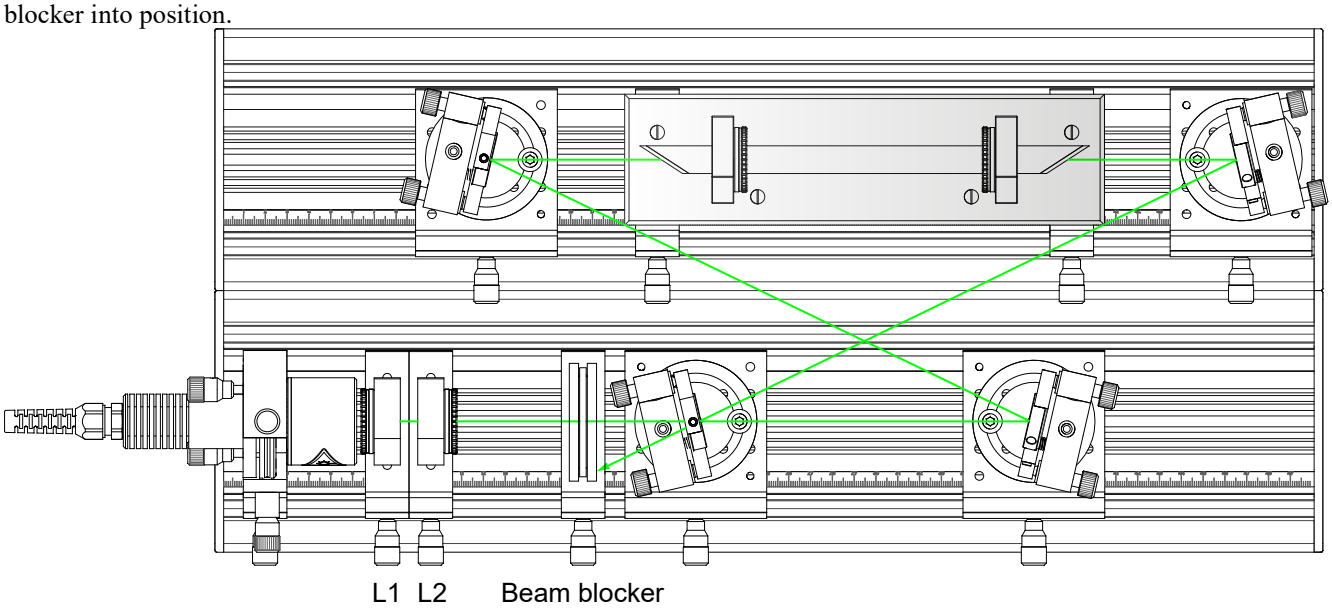

Set now the laser to 350 mA (40 mW) and the temperature for the maximum fluorescence. When striking the correct temperature, the florescence increases and the dimer laser flashes up! After reaching the optimum temperature of the pump laser, the iodine ring laser permanently oscillates, however you will notice fluctuation of the lasing wavelength (greenish yellow, yellow, red, dark red) as well of the mode structure. To improve the laser oscillation, L2 may be moved forth and back. ...and not to forget, the Brewster windows needs to be cleaned with the provided optics cleaning kit. From time to time also the resonator mirror should be cleaned.

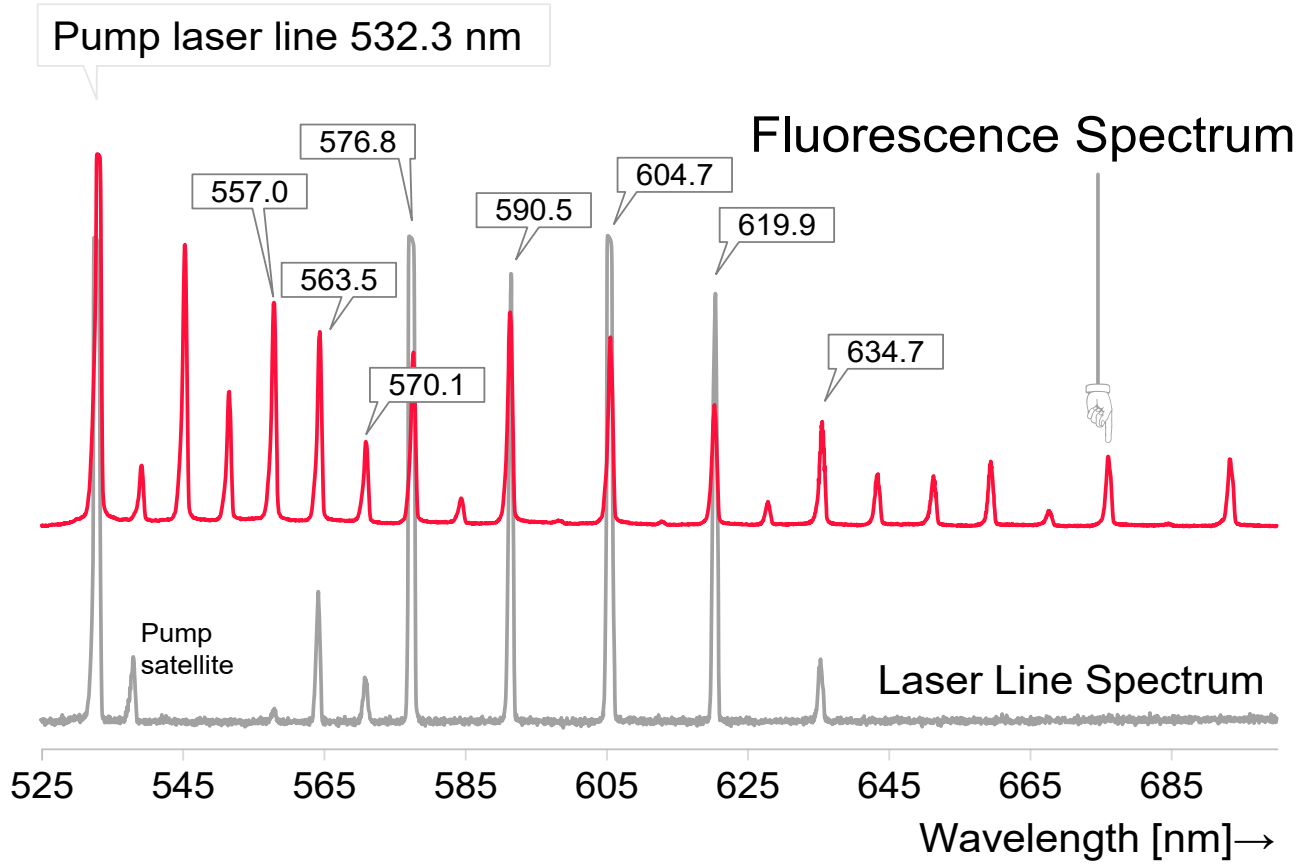

Fig. 2: Measured multi line spectrum

3.7 Laser Line Tuning

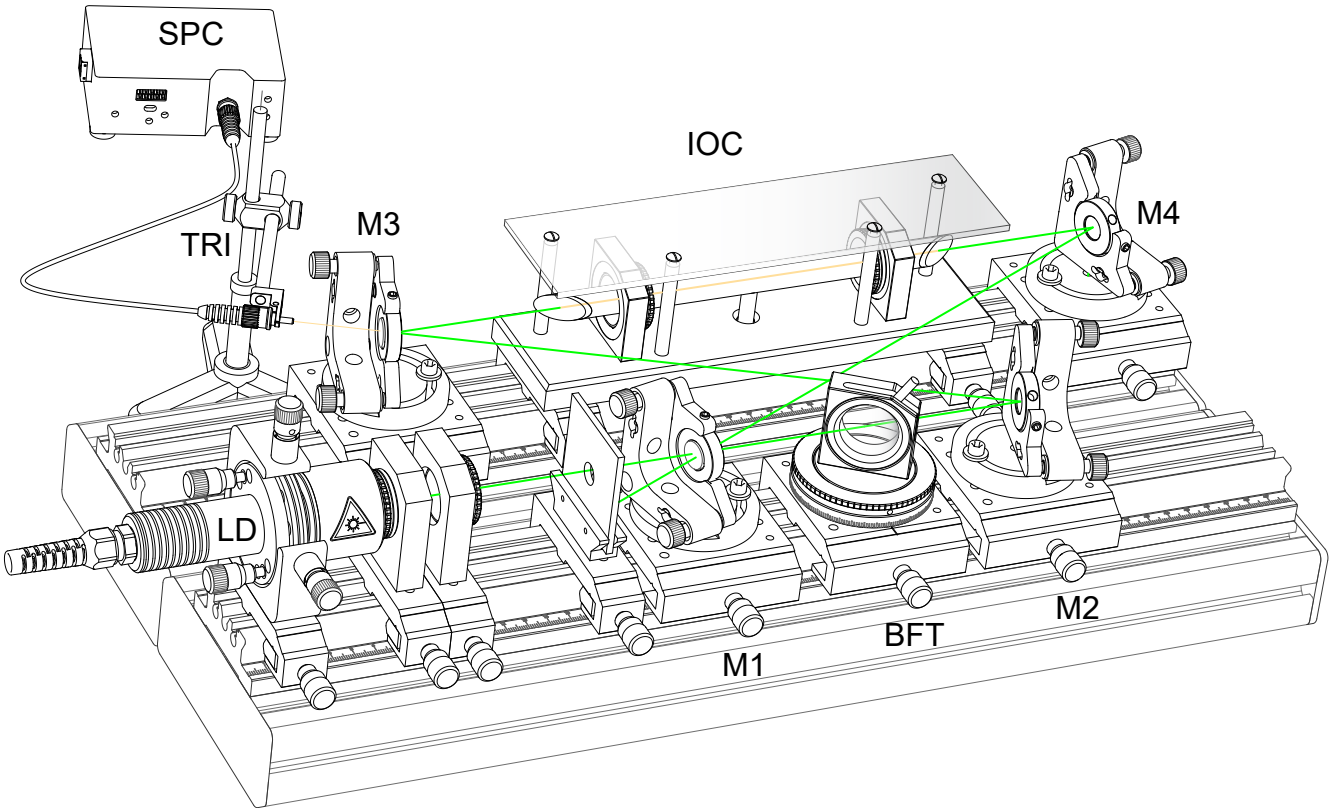

When the iodine laser is optimised with respect to the temperature of the pump laser and ring laser alignment, the birefringent tuner (BFT) may be inserted. Before so, make sure, that the BFT tuner is set to the Brewster angle (57°). When the ring laser stops oscillating, rotate the birefringent plate with the lever around its optical axis. At least a strong line will oscillate. The BFT causes a slight beam offset, which requires realigning of the ring laser. The oscillation of a single laser line is verified using a spectrometer or the provided transmission grating.

3.8 Hyper Fine Laser Lines

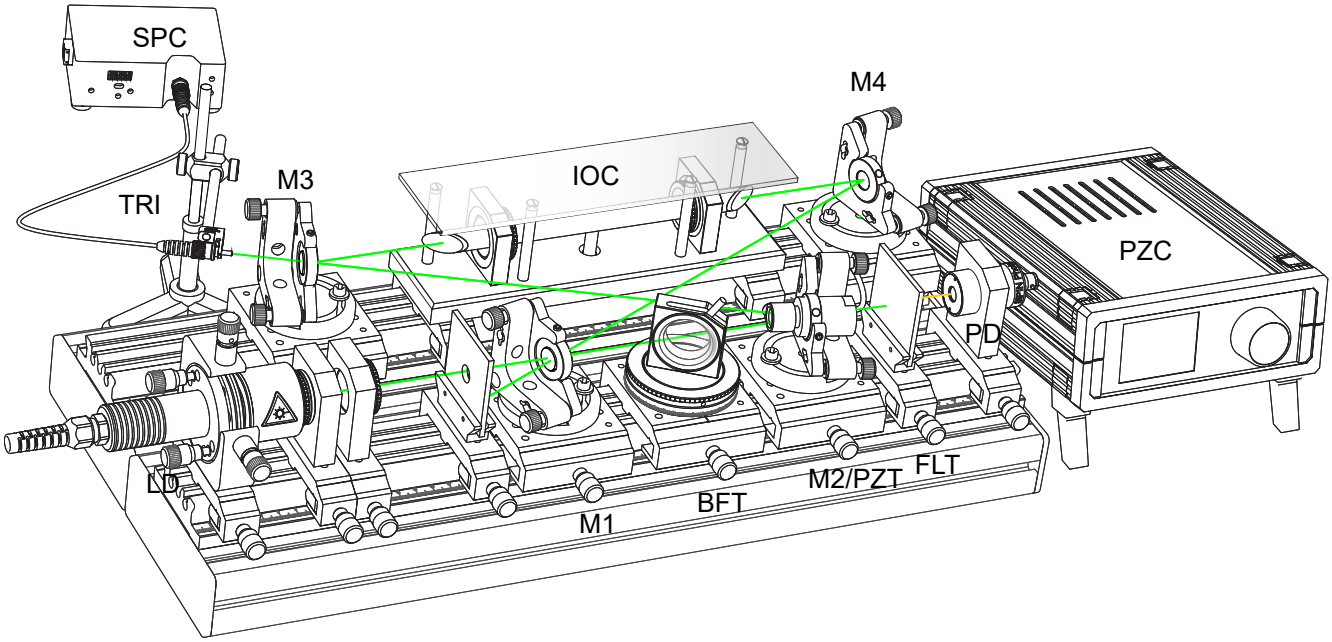

The mirror of M2 is attached to a PZT which is fixed to the mirror adjustment holder M2. The piezo element is controlled by the PZC controller and the ring laser output is measured with the photodiode PD. The PD is connected to the signal box ZB1 where the photo current is converted to a linear voltage which may be displayed on an oscilloscope. A filter (FLT) located in front of the photodetector blocks the pump laser radiation of 532 nm.

Required equipment

Piezo controller 0-50V

This controller provides the voltages necessary for the supply of the Piezo element and the monitor signals. The output voltage may be adjusted from 1 to 50 V and the frequency of the integrated modulator for triangular signals up to 100 Hz. A monitor signal, which is proportional to the selected Piezo voltage is provided via a BNC panel jack at the rear. The controller is equipped with a touch panel display and with digital knob to selected and set the parameter.

To move the Piezo element periodically forth and back (to scan the Fabry Perot mirror spacing) a linear triangle shaped voltage is required. This voltage is characterised by the amplitude and its bias. The frequency should be chosen such, that a flicker free trace on the oscilloscope is achieved, a value of below 100 Hz is fully sufficient.

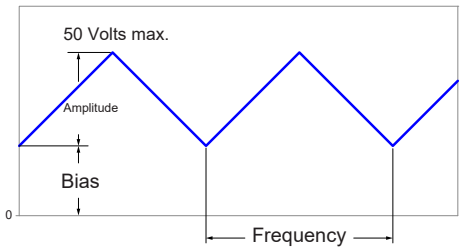

After switching on the controller, the main screen appears. To continue it is required to touch the screen.

The upcoming screen provides three touch buttons:

1. Piezo Settings
2. Ramp Generator
3. Device Info

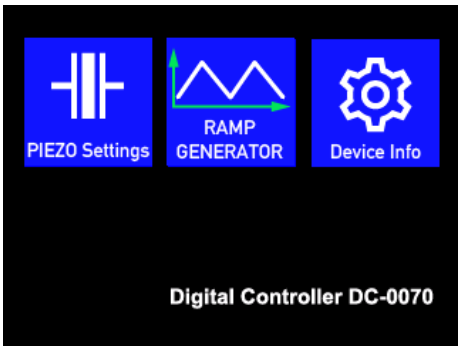

Within the “Piezo Settings” screen the piezo voltage can be switched ON or OFF. Touching the display area of the “Amplitude” it is highlighted and with the setting knob the desired value is chosen.
Touching the “BIAS VOLTAGE” display area activates the setting for this parameter.

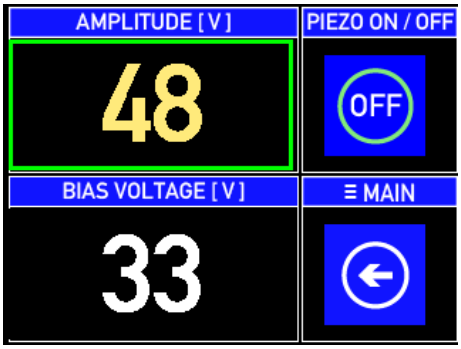

Touching the “Ramp Generator” button brings up the settings screen. Touching the “SCAN FREQUENCY” display area highlights it and allows the setting of the modulation frequency in a range from 1 to 100 Hz. Activating the “RAMP AMPLITUDE” display area allows the setting of the amplitude of the triangular voltage applied to the Piezo element.

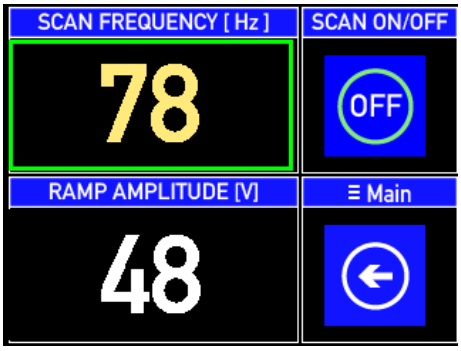

Si PIN photodetector module (PD)

A Si PIN photodiode is integrated into a 25 mm housing with two click grooves (PD). A BNC cable and connector is attached to connect the module to the photodetector signal box ZB1. The photodetector module is placed into the mounting plate (MP) where it is kept in position by three spring loaded steel balls.

Parameter	Symb.	Value	Unit
Rise and fall time of the photo current at: R_L=50Ω; V_R=5 V; λ=850 nm and I_p=800 µA	t_r, t_f	20	ns
Forward voltage I_F = 100 mA, E = 0	VF	1.3	V
Capacitance at V_R = 0, f = 1 MHz	C_0	72	pF
Wavelength of max. sensitivity	λ_{Smax}	850	nm
Spectral sensitivity S 10% of S_{max}	λ	1100	nm
Dimensions of radiant sensitive area	L × W	7	mm^2
Dark current, V_R = 10 V	IR	≤ 30	nA
Spectral sensitivity, λ = 850 nm	S(λ)	0.62	A/W

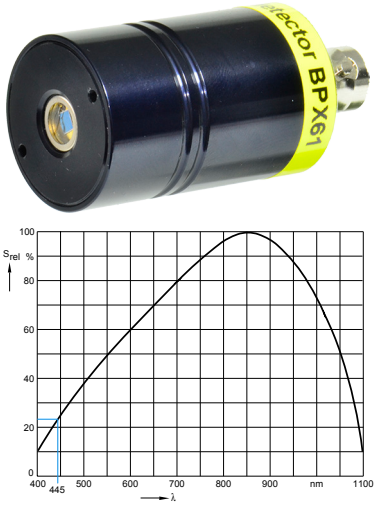

Fig. 3: Sensitivity curve $S_{rel}(\lambda)$

Photodetector Signal Box ZB1

The signal box contains a resistor network and a replaceable 9V battery and is prepared to accept all kinds of photodiodes provided they are connected to the BNC input (PD_{IN}) (see Fig. 5). At the output PD_{OUT} of the signal box a signal is present which is given by the following equation:

$$I_P = \frac{U_m}{R_L}$$

I_P is the photo current created by illuminating the photodiode with light.
U_m is the voltage drop across the selected load resistor R_L.
To convert the measured voltage into a respective optical power we need to involve the spectral sensitivity S(λ) [A/W] which depends on the wavelength of the incident light according to Fig. 3. The detected optical power P_{opt} in W can be given as:

$$P_{opt} = \frac{I_p}{S(\lambda)}$$

Assuming a wavelength of 700 nm we take the value of S_{rel} from Fig. 3 as 0.8 and subsequently the value of

$S(\lambda=700nm)$ is 0.62 x 0.8 = 0.496

If we are measuring a voltage U_m of 1V with a selected resistor R_L of 1K the optical power will be

$$P_{opt} = \frac{I_p}{S(\lambda)} = \frac{U_m}{R_L \cdot S(\lambda)} = \frac{5}{1000 \cdot 0.496} = 10\,mW$$

It must be noted that the measured power is correct only if the entire light beam hits the detector.

Fig. 4: Photodetector signal box

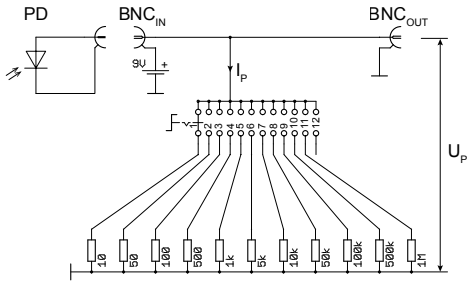

Fig. 5: Photodetector signal box schematic

Based on the selected load resistor the sensitivity will be high for higher resistors but the rise and fall time will be longer. For fast signals a low resistor should be used, however the sensitivity will be lower.

With the piezo element (PZT) which is connected to the ramp voltage generator (PZC), the length of the ring laser is changed periodically. As a result of this, the resonance frequency of the resonator is changed accordingly like a Fabry Perot. If the resonance frequency coincides with a laser transition, laser oscillation on this frequency takes place.

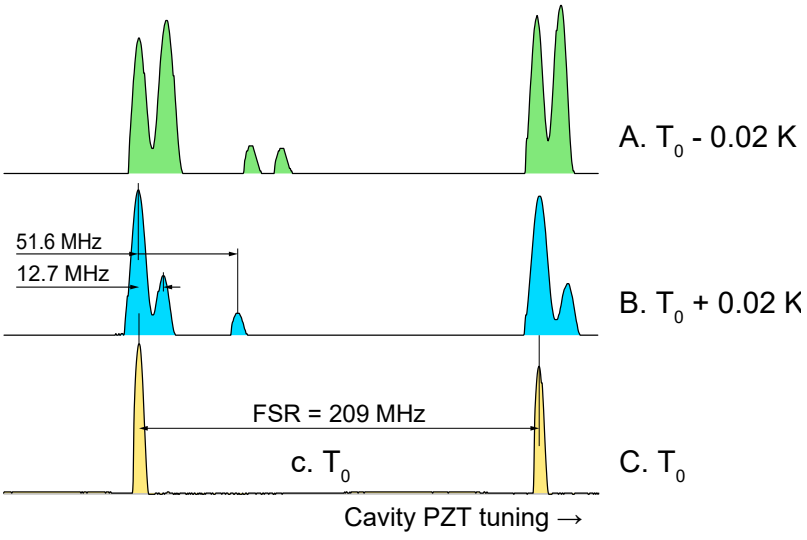

Fig. 6: Scanning profiles of the iodine ring laser

The scanning profiles of Fig. 6 have been recorded in this way. From the theoretical considerations we know, that the iodine ring laser operates in single mode only due to the coherent coupling to the pump field. The profile (C.) shows a "Fabry Perot" like single mode scan. The geometry of the ring laser results in a free spectral range of 209 MHz and the temperature of the pump laser was T_0. By slightly changing the temperature (frequency) a series of additional peaks arose. Since the spectral spacing is very small compared to vibrational levels, these peaks can be related to hyperfine laser transitions.

4.0 Bibliography

1. D. Brewster, “Observations on the Lines of the Solar Spectrum and on those produced by the Earth’s Atmosphere, and by Action of Nitrous Acid Gas”, Trans. Roy. Soc. (Edinburgh) **12**, 519 (1834)
2. Molecular Physics, Wolfgang Demtröder, 2005 WILEY-VCH
3. Von Jan Homann - Eigenes Werk, CC BY-SA 3.0, https://commons.wikimedia.org/w/index.php?curid=6504291
4. B. Wellegehausen, IEEE Journal of Quantum Electronics, QE-15, (1979) 1108-1130.
5. B. Wellegehausen, K. H. Stephan, D. Friede, and H. Welling, “Optically pumped continuous I_2 molecular laser,” Opt. Commun, vol. 26, pp. 391-395, Sept. 1977
6. J.B. Koffend and R.W. Field, “CW optically pumped molecular iodine laser”, J. Appl. Ohys., vol 48, pp 4468-4472, Nov 1977.
7. V. V. Raman and K. S. Krishnan, “A new type of secondary radiation”, Nature 121, 501 (1928)
8. B.Struve, W.Luhs, G.Litfin, Crystal optics and its importance in laser technology, Year book for optics and precision mechanics 1989
9. W. Luhs, B. Struve, G. Litfin, Tunable multi lines He-Ne laser, Laser and Optoelectronics, 4. 1986, AT-Fachverlag GmbH Stuttgart
10. W. W. Rigrod, "The optical ring resonator," in The Bell System Technical Journal, vol. 44, no. 5, pp. 907-916, May-June 1965.
11. H. Kogelnik and T. Li, “Laser beams and resonators”, Appl. Opt. 5 (10), 1550 (1966)
12. Townes, C.H. ; Schawlow, A.L.: Microwave spectroscopy. New York : Dover, 1975
13. Broyer, M. ; Vigue, J. ; Lehmann, J.C.: Effective hyperfine Hamiltonian in homonuclear diatomic Molecules. Application to the B state of molecular iodine. In: J. de Phys. 39 (1978), S. 591